

AD-A267 382

SECURITY CLASSIFICATION OF THIS PAGE



REPO

Form Approved
OMB No. 0704-0188

1a. REPORT SECURITY CLASSIFICATION Unclassified	1b. RESTRICTIVE MARKINGS None
2a. SECURITY CLASSIFICATION AUTHORITY DTIC ELECTED	3. DISTRIBUTION/AVAILABILITY OF REPORT Approved for public release: Distribution unlimited
2b. DECLASSIFICATION/DOWNGRADING SCHEDULE SCHEDULE 7 1993	4. PERFORMING ORGANIZATION REPORT NUMBER AFOSR-0253-89-F
5. MONITORING ORGANIZATION REPORT NUMBER(S) AFOSR-TR-89-0181	

6a. NAME OF PERFORMING ORGANIZATION University of Nebraska-Lincoln	6b. OFFICE SYMBOL (if applicable) NE	7a. NAME OF MONITORING ORGANIZATION AFOSR/NE								
6c. ADDRESS (City, State, and ZIP Code) Office of Sponsored Programs University of Nebraska-Lincoln Lincoln, Nebraska 68588-0511	7b. ADDRESS (City, State, and ZIP Code) 110 Duncan Avenue, Ste B115 Bolling AFB, DC 20332-0001									
8a. NAME OF FUNDING/SPONSORING ORGANIZATION AFOSR/NP	8b. OFFICE SYMBOL (if applicable) NE	9. PROCUREMENT INSTRUMENT IDENTIFICATION NUMBER Grant No. AFOSR-89-0253								
8c. ADDRESS (City, State, and ZIP Code) 110 Duncan Avenue, Ste B115 Bolling AFB, DC 20332-0001	10. SOURCE OF FUNDING NUMBERS <table border="1" style="width: 100%; border-collapse: collapse; margin-top: 5px;"> <tr> <th style="width: 25%;">PROGRAM ELEMENT NO.</th> <th style="width: 25%;">PROJECT NO.</th> <th style="width: 25%;">TASK NO.</th> <th style="width: 25%;">WORK UNIT ACCESSION NO.</th> </tr> <tr> <td style="text-align: center;">61102F</td> <td style="text-align: center;">2301</td> <td style="text-align: center;">A7</td> <td></td> </tr> </table>		PROGRAM ELEMENT NO.	PROJECT NO.	TASK NO.	WORK UNIT ACCESSION NO.	61102F	2301	A7	
PROGRAM ELEMENT NO.	PROJECT NO.	TASK NO.	WORK UNIT ACCESSION NO.							
61102F	2301	A7								

11. TITLE (Include Security Classification)
 Surface Flashover of Semiconductors: A Fundamental Study (U)

12. PERSONAL AUTHOR(S)
 P.F. Williams and W.C. Nunnally

13a. TYPE OF REPORT Final	13b. TIME COVERED FROM 1/15/89 TO 1/14/93	14. DATE OF REPORT (Year, Month, Day) 1993, June 16	15. PAGE COUNT
-------------------------------------	---	---	-----------------------

16. SUPPLEMENTARY NOTATION

17. COSATI CODES <table border="1" style="width: 100%; border-collapse: collapse; margin-top: 5px;"> <tr> <th style="width: 33%;">FIELD</th> <th style="width: 33%;">GROUP</th> <th style="width: 33%;">SUB-GROUP</th> </tr> <tr> <td> </td> <td> </td> <td> </td> </tr> <tr> <td> </td> <td> </td> <td> </td> </tr> </table>	FIELD	GROUP	SUB-GROUP							18. SUBJECT TERMS (Continue on reverse if necessary and identify by block number) Surface flashover semiconductor, photoconductive switch
FIELD	GROUP	SUB-GROUP								

19. ABSTRACT (Continue on reverse if necessary and identify by block number)

This report presents research results and activities carried out during the period January 15, 1989 through January 14, 1993 sponsored by AFOSR Grant No. AFOSR-89-0253. Work was carried out at the University of Nebraska (UNL), and at the University of Texas at Arlington (UTA). The work at each of these locations is discussed in detail in separate sections of this report. Important conclusions are: 1) The phenomenon commonly referred to as "surface" flashover in silicon results from a sequence of events occurring primarily inside the silicon, rather than in the ambient surrounding it; 2) Current filamentation plays an important role in the breakdown process; 3) Contacts to the silicon influence the breakdown process; 4) The condition of the sample surface strongly influences breakdown; 5) Flashover can be inhibited through the action of weak visible or near infra-red illumination; 6) Current before the initiation of flashover is strongly space-charge limited; 7) Double injection effects are clearly present in p⁺-i-n⁺ structures, and will limit the applicability of such structures as photoconductive switches.

20. DISTRIBUTION/AVAILABILITY OF ABSTRACT <input checked="" type="checkbox"/> UNCLASSIFIED/UNLIMITED <input checked="" type="checkbox"/> SAME AS RPT. <input type="checkbox"/> DTIC USERS	21. ABSTRACT SECURITY CLASSIFICATION Unclassified
22a. NAME OF RESPONSIBLE INDIVIDUAL Dr. Robert J. Barker	22b. TELEPHONE (include Area Code) (202) 767-5011
22c. OFFICE SYMBOL AFOSR/NE	

**FINAL REPORT
SURFACE FLASHOVER OF SEMICONDUCTORS: A FUNDAMENTAL STUDY
AFOSR-89-0253**

Covering period January 15, 1989 to January 14, 1993

P.F. Williams
*Department of Electrical Engineering
University of Nebraska-Lincoln
Lincoln, NE 68588-0511*

and

W.C. Nunnally
*Applied Physical Electronics Research Center
Box 19380
The University of Texas at Arlington
Arlington, TX 76019-0380*

ABSTRACT

This report presents research results and activities carried out during the period January 15, 1989 through January 14, 1993 sponsored by AFOSR Grant No. AFOSR-89-0253. Work was carried out at the University of Nebraska (UNL), and at the University of Texas at Arlington (UTA). The work at each of these locations is discussed in detail in separate sections of this report. Important conclusions are: 1) The phenomenon commonly referred to as "surface" flashover in silicon results from a sequence of events occurring primarily inside the silicon, rather than in the ambient surrounding it; 2) Current filamentation plays an important role in the breakdown process; 3) Contacts to the silicon influence the breakdown process; 4) The condition of the sample surface strongly influences breakdown; 5) Flashover can be inhibited through the action of weak visible or near infra-red illumination; 6) Current before the initiation of flashover is strongly space-charge limited; 7) Double injection effects are clearly present in p^+i-n^+ structures, and will limit the applicability of such structures as photoconductive switches.

93-16873



1. OBJECTIVES AND MAJOR CONCLUSIONS

1.1 Objectives

The overall objective of the effort is to determine at as basic a level as possible the physical mechanisms responsible for inducing surface flashover in semiconductors, particularly silicon. In order to achieve this objective we set several secondary objectives. These are:

1. The design, construction, and testing of facilities which will allow us to determine experimentally the behavior of semiconductors during a flashover event;
2. The acquisition of empirical data which clarify the sequence of events occurring during flashover;
3. The interpretation of these data in terms of the basic physical processes occurring in the sample.

Research was conducted at two locations: the University of Nebraska-Lincoln (UNL), and the University of Texas at Arlington (UTA). Because different approaches were used by the two groups, the specific activities of the two groups in pursuit of these objectives differed. These are summarized in the next section, and described in full detail in the following two chapters.

1.2 CONCLUSIONS

University of Nebraska

Among the conclusions of the work at UNL are the following.

1. Surface flashover of silicon $p^+ - i - n^+$ structures is a result primarily of processes occurring inside the silicon rather than outside it. This is an important result because it shows that conventional models developed to understand surface flashover of insulators should not be applicable to these structures.
2. Current constriction plays an important role in the overall flashover process.
3. At a given voltage, flashover can be inhibited or delayed in several ways.
 - a. Weak illumination of the sample can inhibit flashover of $p^+ - i - n^+$ structures.
 - b. Flashover delay for $n^+ - i - n^+$ structures is considerably longer than for $p^+ - i - n^+$ structures.
 - c. Flashover can be inhibited by etching grooves into the surface of the silicon sample
 - d. Flashover can be inhibited by making a laminated structure consisting of several stacked thin layers instead of a single piece of silicon of the same length. For $n^+ - i - n^+$ structures very little

improvement was noted, but for p^+i-n^+ structures substantial inhibition was observed. Double injection effects limit the utility of these structures, however.

University of Texas at Arlington

Accomplishments at the University of Texas at Arlington include the following.

1. An experimental technique to measure the surface electric fields on semi-conductors was designed and implemented. The temporal resolution of the technique was improved to about 20 ns, and the spatial resolution was 50 μm . In the course of developing the facility, it became necessary to measure the electro-optic coefficient of nitrobenzene, and an empirical value for this datum was determined.
2. This facility was used to measure surface electric fields for a number of samples with aluminum and gold contacts. Effects of processing variations such as anneal method (rapid thermal or furnace) were tested. It was found that the surface electric fields showed spatial non-uniformity at all fields, and temporal non-uniformity at the higher applied voltages. Evidence of surface charging was observed as indicated by the presence of electric field after the voltage pulse was removed. Although both furnace and rapid thermal annealing seemed to produce about the same flashover characteristics, furnace annealing seemed to produce more uniform pre-breakdown surface fields.
3. Various contact materials and processing methods were used to determine effects on flashover characteristics. The flashover threshold was observed to be the highest for unannealed aluminum contacts (40-45 kV/cm). The next best results were obtained with unannealed gold contacts (2500 \AA gold and 500 \AA titanium for proper adhesion) which had a flashover threshold of 35-40 kV/cm. In some samples, the post-breakdown electric fields were observed to be higher than the pre-breakdown electric fields for the same applied voltage. Hence surface charge, contact material and contact annealing play an important role in influencing the breakdown/flashover properties.

1003

Accession For	
NTIS - CRA&I	<input checked="" type="checkbox"/>
DTIC - TAB	<input type="checkbox"/>
Unannounced	<input type="checkbox"/>
Justification	
By	
Distribution /	
Availability Codes	
Dist	Avail and/or Special
A-1	

2. WORK AT THE UNIVERSITY OF NEBRASKA-LINCOLN

2.1 General Experimental Information

All experimental work done at UNL has emphasized minimizing complications in interpreting empirical results. For that reason, we have concentrated on studying silicon structures with diffused n^+ and p^+ contacts, and have carried out our flashover experiments in a vacuum.

2.1.1 Experimental Setup

Fig. 2-1 shows the experimental setup used for all the empirical results reported

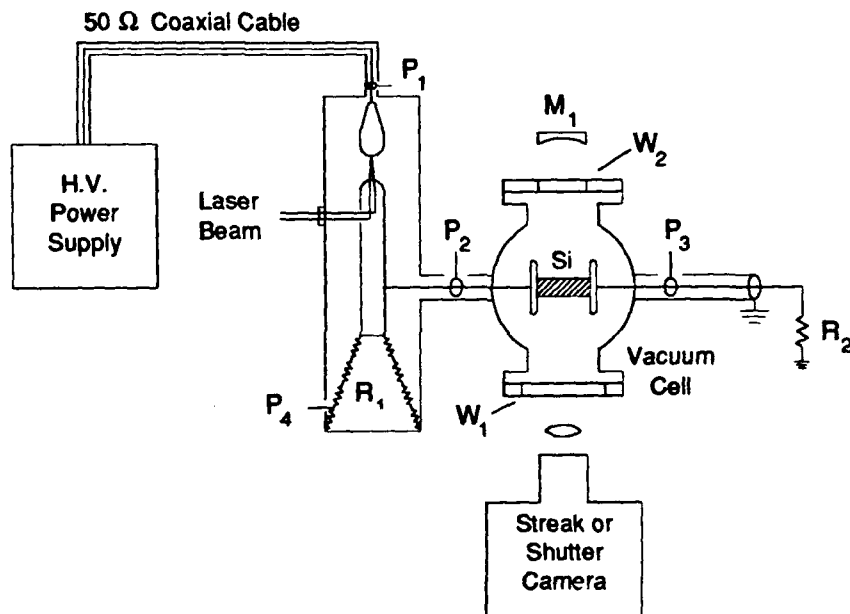


Figure 2-1. Schematic diagram of the experimental setup.

here. Voltage is applied to the sample in pulses. The pulse generator portion of the system consists of a charged $50\ \Omega$ coaxial cable which is switched to the load with a laser-triggered spark gap. Both a Q-switched Nd:YAG laser and a N_2 laser have been used for triggering. The coaxial cable is connected to a regulated high-voltage power supply, and can be charged to any voltage up to 70 kV. Generally the load consisted of a matched $50\ \Omega$ load resistor in parallel with the sample under test. As long as the current in the sample is small in comparison to the load current, the generator in this configuration produces clean, rectangular pulses of voltage half the charging voltage, and duration determined by the length of the charged coaxial cable. For all experiments reported here which utilize this configuration, this length was such as to produce pulses 290 ns long, and the rise and fall times were about 15 ns. The maximum voltage we were able to apply with this configuration was 35 kV.

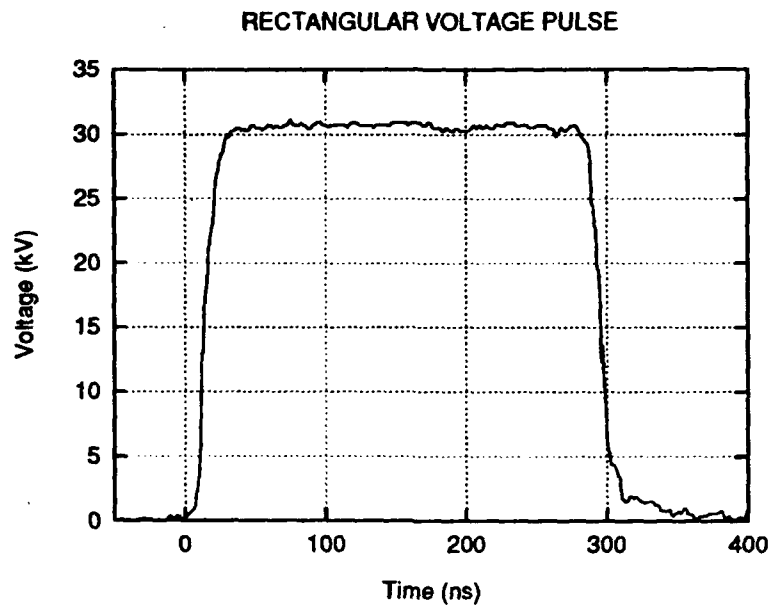
The generator can also be operated with a load resistance greater than that of the charged coaxial cable. For large values of load resistance, it produces pulses with peak magnitude equal to the charging voltage, and a nearly exponential decay with time constant determined by the resistance. Superimposed on the exponential decay are a damped sequence of 30-40 ns wide, low-going pulses produced by the initial switching transient. The pulses are spaced by the round trip transit time for the charged coaxial cable. Figs. 2-2 show the voltage pulses obtained in both configurations.

Samples generally consisted of rectangular prisms with dimensions of about $10 \times 8 \times 2.5$ mm, and voltage was applied across the long (10 mm) dimension of the sample. A more detailed description of the samples and of their preparation is given in the next section. The sample was mounted in a chamber which could be evacuated to a pressure less than 10^{-6} Torr using a turbo-molecular pump. One end of the sample was connected to the high voltage generator and the other was connected to a 50Ω resistor, via a length of 50Ω , RG8/U cable. Voltage diagnostics consisted of capacitively-coupled probes, labeled P_2 and P_3 in the figure which measure the voltage on both sides of the sample, and of a 20.5Ω current-viewing resistor in series with the matched 50Ω load labeled P_4 . The sample current could be obtained by dividing the voltage at P_3 by the 50Ω resistance of the terminated coaxial cable. Voltage traces from a Tektronix 7104 oscilloscope were captured digitally using a Tektronix DCS01 camera system, providing storage of single shot waveforms at probe limited risetimes (1-3 ns).

Optical access to the front and back of the sample was provided by windows on opposite sides of the vacuum chamber. The sample was mounted such that the largest faces (10×8 mm) of the sample were parallel to the two windows. Optical diagnostics included a Hamamatsu Model C979 streak camera, and a locally-constructed, image-intensifier-based shutter camera. Both cameras were capable of near-single-photon sensitivity. The minimum time resolution for the streak and shutter cameras were about 100 ps, and 5 ns. The shutter camera did not have framing capability, so only a single photograph could be obtained from a given shot. Both cameras were capable of near single-photon detection sensitivity. The shutter camera had a minimum shutter time of about 5 ns. The time resolution of the streak camera depended on the streak speed and the width of the entrance slit, and varied from less than 1 ns to about 15 ns. The time scales of the electrical and optical diagnostics could be synchronized to within about ± 1 ns, but in many cases the effective time synchronization was limited by the temporal resolution of the camera.

In some experiments a spherical mirror was placed behind the sample chamber so that it produced an image of the rear face of the sample in the plane of the front face of the sample, and just below the sample. With this arrangement, we could obtain simultaneously shutter and streak photographs of events occurring on both large faces of the sample. The mirror image was inverted, however. The effective optical aperture for all photos was determined by the focusing lens, and was $f/8$.

a)



b)

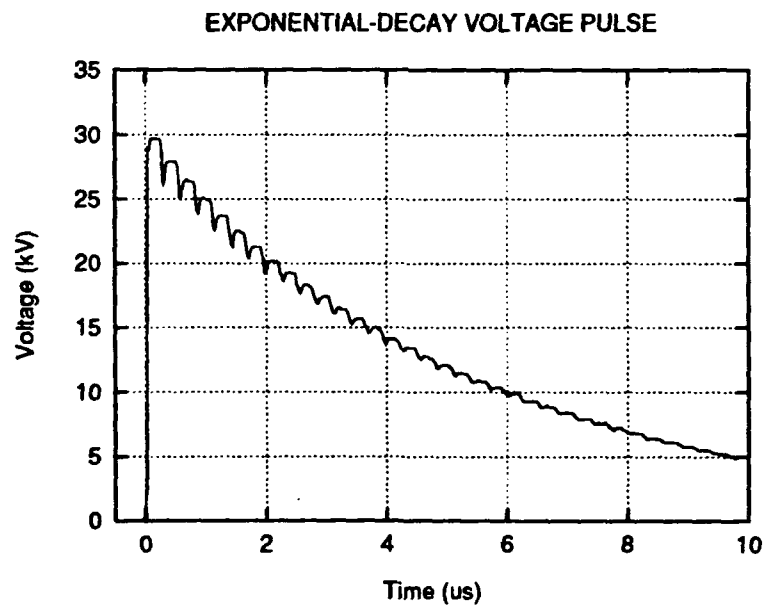


Figure 2-2. Voltage pulses produced by the system: a) with the matched $50\ \Omega$ load resistor, and b) with a $2\ \text{k}\Omega$ load resistor.

2.1.2 Sample Preparation

For all results reported here the samples were rectangular prisms of high resistivity silicon. Samples were fabricated from three different boules of silicon. The resistivity as measured with a four-point probe of one boule was $1.3 \text{ k}\Omega\text{-cm}$ and it was n-type. The resistivity of the other two boules was about $15 \text{ k}\Omega\text{-cm}$, and we could not determine directly whether the material was n or p-type because of the very small carrier density. Measurements made with p^+i-p^+ structures using this material indicate indirectly that it was also n-type. The boules were 1 inch in diameter. Sample fabrication started with cutting a 1 cm thick slice from the boule using a diamond saw. (This step was bypassed for the $1.3 \text{ k}\Omega\text{-cm}$ material because it was obtained from the supplier already cut into 1 cm thick pieces.) The cut faces were ground flat, chemo-mechanically polished using a standard colloidal silica solution, etched in HF to remove oxides, washed in deionized water, and blown dry with nitrogen. This treatment produced flat, mirror-like surfaces which should be relatively damage free. There was a slight rounding of the edges.

Either p^+ or n^+ layers were then diffused into the faces. This was accomplished by using a commercial spin-on dopant source, and then diffusing the source into the sample by heating it to 1150°C for 2 hours in a furnace in flowing N_2 . Boron was used for the p-type impurity, and phosphorus for the n-type. This procedure produced impurity levels exceeding 10^{18} cm^{-3} in a layer several μm thick. After cleaning the samples in an HF solution, they were cut to approximate size using a diamond saw, ground, polished, and cleaned on all four cut sides as described above. To make external contact, a film of aluminum 2500 \AA thick, followed by a 5000 \AA thick film of copper were thermally evaporated onto the diffused faces. Some samples were indium soldered to steel buttons, whereas for others a pressure contact was used.

2.1.3 Contact Characterization

Because our experiments have shown that the contacts play an important role in the flashover phenomenon, we have made a substantial effort to characterize and understand the contacts we form. It appears that our contacts behave mostly as expected, but there are some anomalies which we do not understand. We do not think that these anomalies affect significantly our flashover measurements.

In order to characterize our contacts, we use four-point probe measurements to determine the sheet resistance of the diffused surface, hot point probe measurements to determine the carrier type, and conventional current-voltage measurements. Typical sheet resistances for both n-type and p-type contacts were about $4 \text{ }\Omega/\text{square}$. We estimate the corresponding impurity densities to be about 10^{20} cm^{-3} . On the basis of published diffusion coefficient data for boron and phosphorus^[1] and the measured diffusion temperature and time, we estimate the thickness of the diffused layer to be about 2-5 μm , depending on the precise diffusion temperature. We checked this estimate by carrying out experiments in which the sheet resistance of the surface was measured after each of a sequence of controlled chemical etches. Each etch removed a known thickness of material, and by measuring the sheet resistance after each etch, a graph of resistivity vs. depth could be generated. The diffusion depths determined by this method were generally consistent with the estimated depths.

In order to characterize better the diffused layers and the metallization contact to them, we have made an extensive set of current-voltage measurements. Fig. 2-3 shows a typical I-V curve for a p^+i-n^+ device with a 1 cm long intrinsic region made from the

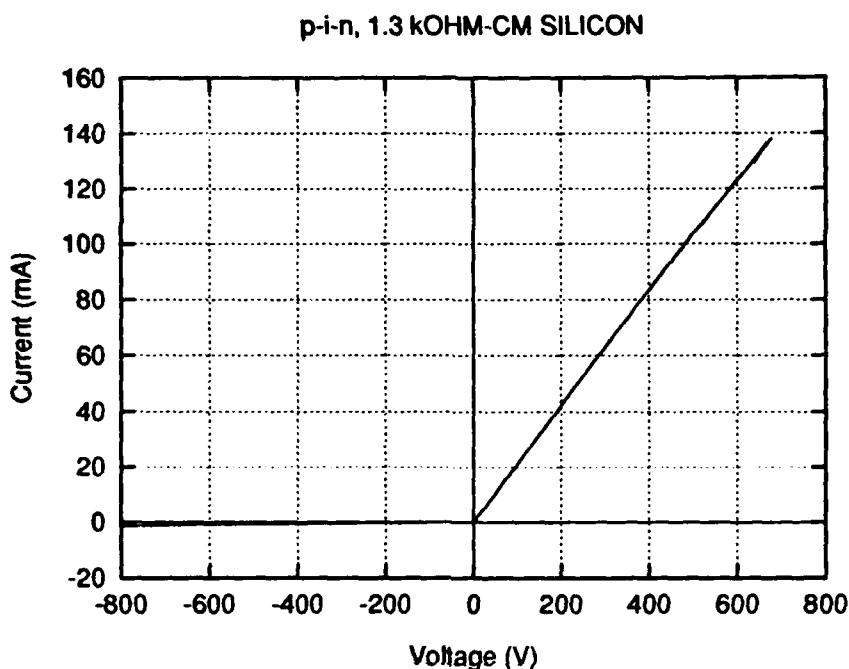


Figure 2-3. A typical I-V curve for a p^+i-n^+ device. The device dimensions were $10 \times 8 \times 2.7$ mm, and voltage was applied across the long dimension. The resistivity of the "intrinsic" material was $1.3 \text{ k}\Omega\text{-cm}$.

$1.3 \text{ k}\Omega\text{-cm}$ silicon. The cross sectional area of the sample was 0.21 cm^2 . With this configuration, both junctions are either forward biased or reverse biased. As expected, the curve is clearly rectifying. In the forward direction, the curve is nearly a straight line with slope corresponding to the resistivity of $1.0 \text{ k}\Omega\text{-cm}$, a little less than the value measured with a four-point probe. In the reverse direction the current is much less than in the forward, but it is at least several orders of magnitude greater than would be expected for a simple reverse-biased junction.^[2]

Fig. 2-4 shows an I-V curve for a similar structure fabricated from a boule of $\sim 15 \text{ k}\Omega\text{-cm}$ material. The characteristic is nearly a straight line in the forward direction, with slope corresponding to a resistivity of $11 \text{ k}\Omega\text{-cm}$, again a little lower than the four-point probe value. As with the $1.3 \text{ k}\Omega\text{-cm}$ device, less current flows in the reverse direction than in the forward, but the current is several orders of magnitude larger than expected.

We believe that the excessive reverse current we observe is due at least in part to damage remaining near the contact surface from the cutting and grinding steps. Devices constructed by doing a deep chemical etch on these surfaces before the final chemical polishing step exhibited reverse currents lower by more than an order of magnitude than

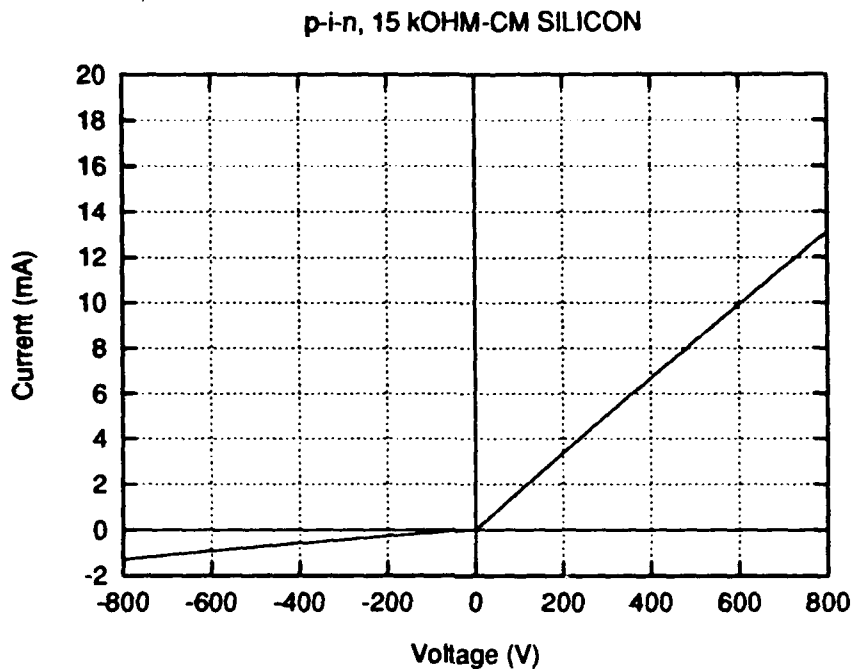


Figure 2-4. Typical I-V curve for a sample similar to that used for Fig. 2-3, except that the resistivity of the base material was $\sim 15 \text{ k}\Omega\text{-cm}$. The sample dimensions were $10 \times 8 \times 2.3 \text{ mm}$.

those fabricated without the chemical etch.

2.2 Flashover Characteristics of $p^+ - i - n^+$ Structures

When a fast-rising voltage pulse is first applied to a $p^+ - i - n^+$ silicon sample, the current which flows is roughly that expected from the bulk sample resistance. After a short time the measured current begins to increase roughly exponentially. The time scale for this increase depends on the condition of the sample surface, and for the samples investigated at UNL it varies between about 10 and several hundred ns, with the shorter time being characteristic of samples that had undergone fewer than ~ 50 shots. Even the longest time scale is much too short to be the result of bulk resistive heating.

Fig. 2-5 shows a sequence of shutter photographs of the emission recorded during flashover, and a typical breakdown current oscillogram for a $p^+ - i - n^+$ sample. The sample had undergone fewer than 30 shots. Except for changes in the delay between the arrival of the voltage pulse and the onset of the rapid current rise signaling breakdown, photos and current traces from samples which had undergone many more shots (up to 1000) were similar. In many cases the "aged" samples developed preferred breakdown paths whereas the breakdown path for "new" samples varied randomly from shot-to-shot. Both front and rear views are shown in Fig. 2-5, with the rear view being inverted by the optical system. The positions of the edges of the sample for both views are indicated in the figure by white dotted lines. The shutter camera was capable of acquiring only one photo at a time, so these photographs are each of a different shot. There was substantial shot-

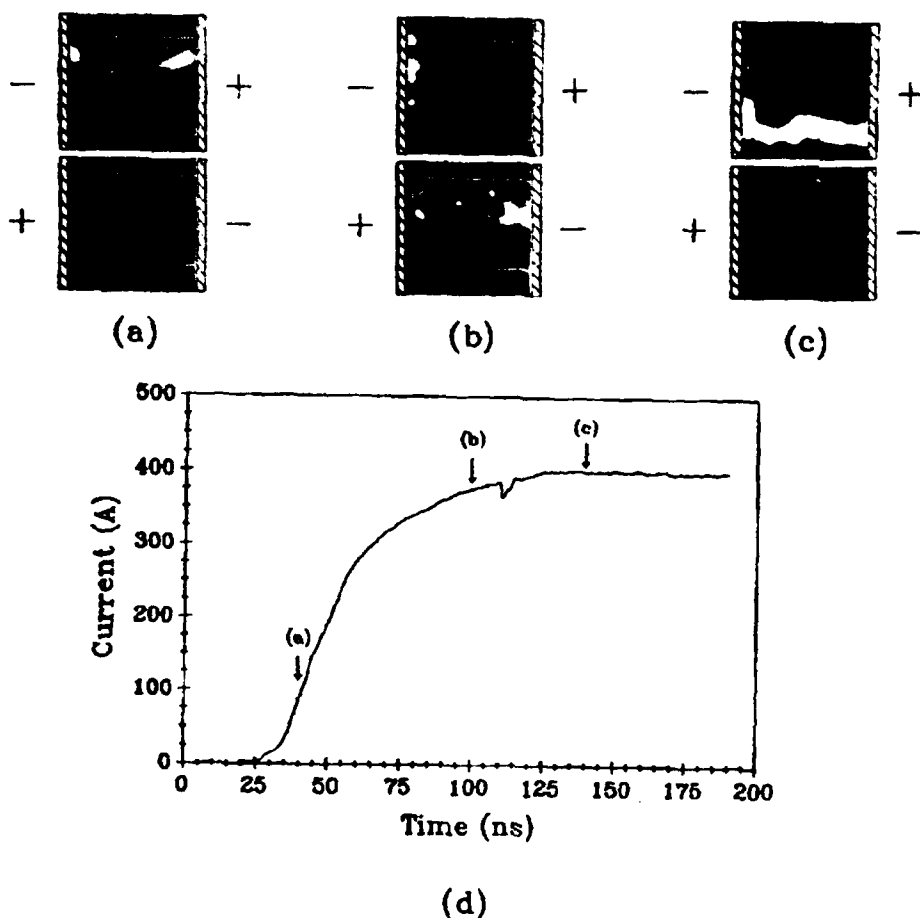


Figure 2-5. Shutter photographs (a, b, and c) and a representative current trace (d) showing the progress of surface flashover in a vacuum ambient on a silicon sample which had undergone < 30 shots. The applied voltage during the pulse was 30 kV across a 1 cm sample. Each photograph is from a different shot, and the current trace is that recorded for the photo in c). The timing of each photo is shown by the vertical arrows in the current trace. A spherical mirror was used behind the sample to provide a simultaneous record of events on both the front and rear faces of the sample. The image from the rear face is inverted. In the photos, the upper photo is from the front face, the lower from the rear. In each photo, the boundaries of the sample are indicated by the white, dotted lines.

to-shot variation, but the photos are representative of the sequence of events. The shutter time was ~ 5 ns, and the time when each photograph was taken is shown in the representative current trace in Fig. 2-5d.

Fig. 2-6 shows streak photographs of two breakdown events. The horizontal dimension of the photos just spans the length of the sample, and time increases downward. In order to see events from the entire surface of the sample, a cylindrical lens was used to focus emission into a narrow, slit-shaped region. Since no entrance slit was used, the time resolution was determined from the dimensions of this region and was about

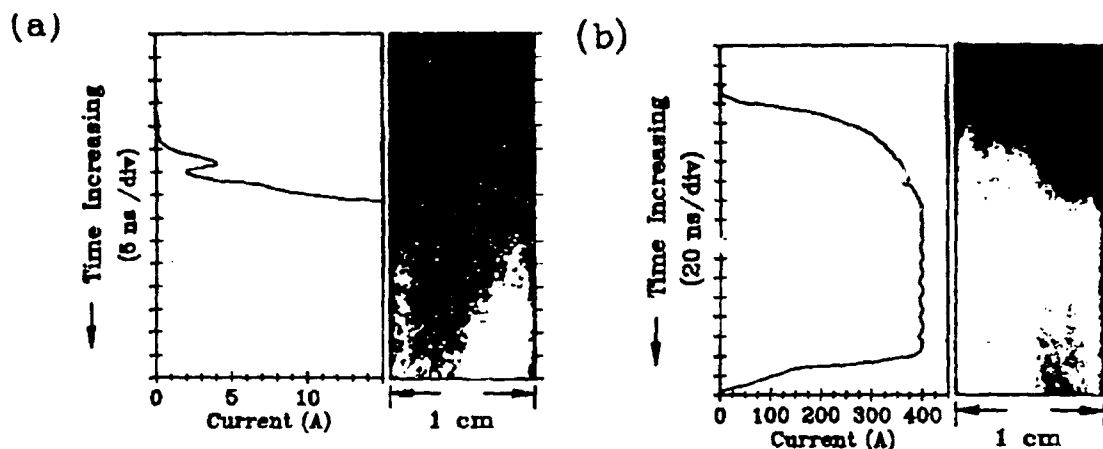


Figure 2-6. Streak photographs and corresponding current traces of two breakdown events. The horizontal axis of the photos corresponds to the spatial dimension along the inter-electrode axis, and the vertical to the temporal dimension, with time increasing downwards. The vertical edges of the photos correspond to the positions of the two contacts to the sample, and a cylindrical lens was used to concentrate emission to a thin line corresponding to $\pm 4\%$, or about 0.7 division on each photo. The timing synchronization between phot and current trace is accurate to within this uncertainty. (a) Streak photo and current trace showing the early stage of breakdown. The white, dotted line is an artifact introduced to help in determining timing synchronization with the current trace. A spherical mirror was used behind the sample to provide a record of events on both faces of the sample simultaneously. Both images were focussed to a single line by the cylindrical lens. The image from the rear surface is inverted, making the front appear to travel in the opposite direction to that which it actually travelled. Fronts are seen on both faces in this photo, both emanating from the cathodic contact (on the left in the photo of the front surface). It is clear that visible emission first appeared some 10-15 ns after the onset of the rapid current rise leading to breakdown. (b) Lower temporal resolution streak photo and current trace showing the entire course of a breakdown event. In this case the rear mirror was blocked, and only emission from the front face is recorded. As in a), the cathodic contact was on the left.

$\pm 4\%$ of full scale or 3.5 and 14 ns for Figs. 2-6a and 2-6b respectively. In Fig. 2-6a a spherical mirror was used behind the sample to record the emission from both broad faces. Since the image of the rear face is inverted, a front moving from left to right appears to move from right to left. This feature helps to separate events occurring on the two faces. In Fig. 2-6b emission is seen from only the front face because the rear mirror was blocked.

The first optical event observable in Figs. 2-5a and 2-6a is a small spot of light appearing near the cathode about 20 ns after the arrival of the voltage pulse at the sample. By reversing the polarity of the applied voltage pulse we verified that the spot is associated with the cathode and not with a specific contact on the sample. In all cases for which we have data, this first emission appeared *after* (typically ~ 10 ns) the start of the rapid current rise signaling breakdown. Within 10-50 ns after the appearance of the cathode spot, emission spreads to other areas of the sample surface, moving roughly as a

wavefront with a speed in the range $1 - 5 \times 10^7$ cm/sec. As seen in Fig. 2-6b, the motion was often sporadic, and the luminosity was non-uniformly distributed across the sample surface. Emission also often appeared in mid gap, initially unconnected to either electrode. Fig. 2-5b shows a shutter photograph of such an event. Shutter photographs such as those shown in Fig. 2-5 show that the emission is localized to one, or at most a few, channels.

From fast photographic results and from post-mortem scanning electron microscope (SEM) photographs, it is clear that current filamentation plays an important role in the flashover event. Damage tracks seen in the SEM photos show clearly that at some time during flashover current flowed in one or more channels only a few μm in diameter. High speed photographs obtained at UNL suggest that one or more thin filaments first form near the cathode during flashover, and then propagate with speeds between 10^7 and 10^8 cm/sec toward the anode. This conclusion is based on the observation of light emission from the sample, and is therefore indirect. Complete breakdown (as evidenced by the device resistance becoming insignificant in comparison with the 50Ω generator resistance) occurs only after the optical emission filament bridges the contacts.

There is a clear "aging" effect in that surface flashover becomes increasingly delayed as the number of flashover events on it increases. This effect is presumably due to surface damage. Scanning electron microscope (SEM) photomicrographs of the surfaces of samples which had undergone several flashover events showed very clear surface damage. It was evident in these samples that melting had occurred in narrow channels in or just under the surface. Dr. M. Pocha at Lawrence Livermore Laboratories used an infrared microscope to search for channels under the surface of one of our samples that had undergone a number of flashover events. There was very little indication that such channels existed, but there was one case in which two roughly co-linear channels visible on the surface in SEM photomicrographs appeared to be connected by a shallow sub-surface tunnel. It is not clear whether the lack of evidence for channels in the silicon bulk indicates that current filamentation occurred only near the surface, or that the channels recrystallize into a form which does not cast a shadow in the infrared photomicrographs.

2.3 Flashover Inhibition

2.3.1 Photo-Inhibition of Flashover

We have found that weak (about $10 \mu\text{J}$) optical illumination can inhibit flashover in $\text{p}^+\text{-i-n}^+$ structures.^[3] Pulses of 10 ns duration of both 532 nm and 1064 nm illumination can cause inhibition, but about 10 times the light energy is required for 532 than for 1064 nm. Timing experiments show that the inhibition mechanism is related to the optical carriers generated by the light, and experiments involving illuminating only selected regions of the sample show that the location where these photo-carriers are generated affects strongly the inhibition.

To investigate this effect, we used an experimental setup shown in Fig. 2-7. The setup was similar to that in Fig. 2-1, except that the laser-triggered spark gap was triggered by a N_2 laser, and either the 1064 nm fundamental or the 532 nm second harmonic of the Nd:YAG laser was used to illuminate the front face of the sample only. The laser

beam was attenuated and then focused onto the sample through a rectangular slit and cylindrical lens, producing an illuminated bar which extended across the full 7 mm width of the sample. The fractional span and position of the bar along the 10 mm length of the sample could be varied by changing the cylindrical lens placement with micropositioning stages. The inset isometric view in Fig. 2-7 shows graphically how the sample was illu-

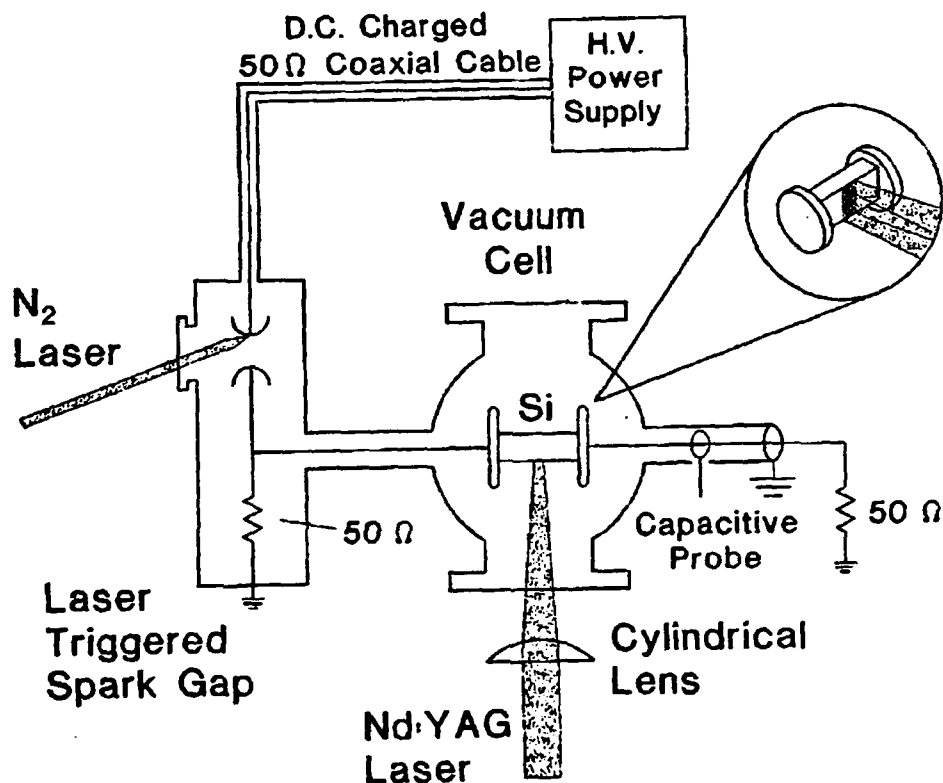


Figure 2-7. Schematic drawing of the experimental setup. The inset shows a detailed isometric view of the illuminated region (shown cross-hatched) on the front surface of the sample.

minated. The total energy of the incident light pulse was attenuated to $10\text{--}100\ \mu\text{J}$ per pulse using wedge beam splitters and neutral density filters. The temporal width of the pulses was about 10 ns.

The flashover-inhibiting effect of weak illumination on p^+i-n^+ structures is shown in Fig. 2-8. The dashed curves show sample current as a function of time without illumination, and the solid curves show similar information, but for the case in which a $18\ \mu\text{J}$ pulse of 1064 nm light illuminated the region near the cathode just prior to the arrival of the voltage pulse. Without illumination, surface flashover is initiated within about 20 ns, and the current rises to a circuit-limited 400 A within about 100 ns. The flashover event is associated with visible emission from one or more filaments on the sample surface as discussed in the previous section. With illumination, on the other hand, flashover does not occur. Instead, the current increases slowly, reaching a final value of less than 20 A at

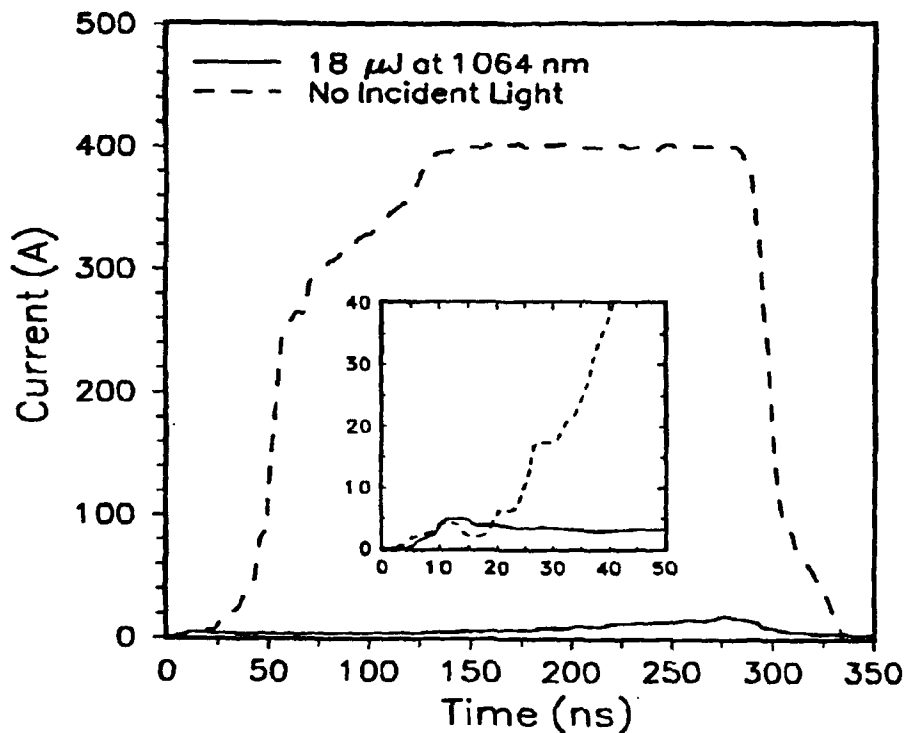


Figure 2-8. Plot of current as a function of time through a silicon sample. The dashed traces represent a typical breakdown event with no light incident on the sample. Solid traces show the current when a 1 mm long region adjacent to the cathode contact was illuminated with a 10 ns, 18 μ W pulse of 1064 nm light applied 120 ns before the voltage pulse. The inset graph shows the behavior at early times on an expanded scale.

the end of the voltage pulse. The data shown in Fig. 2-8 is typical of the current traces seen with several other samples.

The inset in Fig. 2-8 shows the same data on an expanded scale. The arrival of the voltage pulse at the sample is signaled in both curves by a small peak due to capacitive coupling. For a short time thereafter, the current falls to about 2 A, slightly less than expected from the measured low-voltage sample resistance. Without illumination, the current then rises sharply and flashover is initiated. With illumination, this current rise is not seen. After the capacitive pulse the current becomes constant at about 4 A. This current is larger than the minimum current without illumination because of the creation of photo-carriers by the weak illumination.

We carried out several sets of experiments aimed at understanding and documenting the flashover inhibition effect better. Varying the total energy of the light pulse was found to affect the flashover in a quasi-continuous manner. At energies below the value necessary to completely inhibit flashover, the delay to flashover decreased with decreasing pulse energy. Eventually a threshold was reached at which normal flashover delays

occurred, indicating the light was no longer affecting breakdown. The detailed relationship between the illumination energy and flashover inhibition or delay was complex and depended on the position and size of the illuminated region. For the optimum conditions a minimum of about $10 \mu\text{J}$ of 1064 nm illumination was required to suppress flashover.

In another set of experiments, we varied the position and size of the illuminated region. The data shown in Fig. 2-8 was generated by illuminating a strip extending out from the cathode about 1 mm. Fixing the position near the cathode and varying the span of the strip from less than 1 mm up to 4 mm had little effect. When the strip of illumination was moved away from the cathode along the length of the sample, the light was less effective at inhibiting the flashover. Within 1-2 mm of the anode the light no longer delayed flashover at all, and in some cases the flashover risetime (but not the delay to flashover initiation) actually decreased with the application of light at the anode region.

Another set of experiments showed that the photo-carriers produced by the illumination play an important role in flashover inhibition. In these experiments the laser pulse was applied to a 1 mm wide strip just in front of the cathode contact at varied times relative to the voltage pulse. When the laser illumination was applied before the voltage pulse, we found that the light inhibited or delayed flashover when the difference between the two pulses was less than about $20 \mu\text{s}$, comparable to the measured minority carrier lifetime of about $5 \mu\text{s}$ in these samples. The photo-induced pre-flashover current also decreased similarly in these experiments. Flashover could be inhibited when the light pulse was applied after the arrival of the voltage pulse, but only if the light arrived before the sudden current rise signaling the onset of flashover. Once flashover began we saw no cases in which the process was reversed by the application of light.

Results of experiments with light at 532 nm were generally similar to those at 1064 nm, except the energy threshold required to inhibit flashover was about a factor of 10 higher. We also found that even unfocussed light from a simple 40 Watt incandescent table lamp placed about 4 inches from the sample was effective in inhibiting the flashover.

These results are of considerable technological interest because they offer a method for inhibiting the surface flashover of silicon. A practical device incorporating a small incandescent bulb to inhibit flashover of a silicon photo-switch seems feasible. The question of the physical mechanism responsible for the flashover inhibition remains, however. The principal effect of the weak illumination is the generation of free carriers in a surface layer about one absorption length thick. We believe that these carriers are responsible for inhibiting flashover. This conclusion is consistent with our observation that flashover can be inhibited by a light pulse appearing at the sample only within a few minority carrier recombination times of the time of application of the voltage pulse.

The photo-carriers produced by the weak illumination form a plasma capable of shielding its interior from applied fields. The flashover inhibition results reported here suggest that flashover is the result of electric-field-related processes in the region of the cathode, and that the flashover inhibition effect we observe is related to this shielding effect. This suggestion is supported by our observation that even 532 nm illumination will inhibit flashover on all four faces of the sample. The absorption depth of 532 nm

radiation in silicon is only about $1\ \mu\text{m}$, and very few photo-excited carriers should be produced near the rear face of the sample. Further, there is insufficient time for carriers produced on the front face to diffuse to the rear face. Inhibition must, therefore, be the result of a long range effect of the photo-carriers, rather than of the photo-carriers themselves. The shielding field set up by the photo-carriers is the only likely candidate. This is also consistent with results from previous experiments involving time-resolved shutter photography^[4] which showed that in the absence of illumination, flashover seems to be initiated in the cathode region of forward-biased $\text{p}^+\text{-i-n}^+$ structures similar to those discussed here.

The results from the 532 nm illumination also point toward another possible method of inhibiting flashover. Doped regions can easily be diffused into a semiconductor in a controlled fashion to depths on the order of several μm . It might be possible to duplicate the effects of the 532 nm illumination by diffusing a doped layer in a strip near the cathode.

2.3.2 Contact Effects

We have shown that flashover is inhibited in $\text{n}^+\text{-i-n}^+$ structures relative to flashover in $\text{p}^+\text{-i-n}^+$ structures. Most of our experimental work has been with $\text{p}^+\text{-i-n}^+$ devices, but we have also looked at the flashover behavior of $\text{n}^+\text{-i-n}^+$ and $\text{p}^+\text{-i-p}^+$ devices. All devices had high resistivity, $\sim 1\ \text{cm}$ long intrinsic regions. We found that the behavior of the $\text{p}^+\text{-i-p}^+$ devices was very similar to that of $\text{p}^+\text{-i-n}^+$ devices, but that $\text{n}^+\text{-i-n}^+$ devices were able to withstand substantially higher voltages for longer times than were $\text{p}^+\text{-i-n}^+$ devices. Fig. 2-9 shows typical current traces for a $\text{p}^+\text{-i-n}^+$ device and a $\text{n}^+\text{-i-n}^+$ device. The experimental conditions are shown in the caption, and both devices had undergone fewer than 100 shots. With all $\text{p}^+\text{-i-n}^+$ devices we have studied, under these conditions breakdown always started within about 20 ns of the application of the voltage pulse. After many shots (typically more than 100), breakdown would be delayed and in extreme cases would not occur during the 290 ns pulse width, but for relatively "new" samples breakdown always occurred within 20 ns. For the $\text{n}^+\text{-i-n}^+$ samples, however, in more than 20 shots breakdown never occurred during the 290 ns pulse width.

To further study the voltage hold-off capability of a $\text{n}^+\text{-i-n}^+$ sample, we disconnected the matched $50\ \Omega$ load from the spark gap in our pulse generator so that the exponential-decay pulse shown in Fig. 2-2b was produced. In this case, the decay time was about $5\ \mu\text{sec}$. Fig. 2-10 shows the device current when subject to this waveform. The sample withstood the charging voltage for about $1\ \mu\text{sec}$ before breaking down. When operated in this mode, each shot produced substantial sample damage, and after three shots, the current waveform changed to a somewhat broader pulse with peak current about one third of that with the new sample. The delay was also about 200 ns longer.

2.3.3 Surface Morphology Effects

We have also investigated a ribbed device shown schematically in Fig. 2-11. A set of 5 grooves were etched into the surface of a $\text{p}^+\text{-i-n}^+$ device of standard ($\sim 10 \times 8 \times 2.5\ \text{mm}$) dimensions. The grooves were about 1 mm wide and 0.5 mm deep. Upon testing the device, we found that it did not breakdown at all for $5\ \mu\text{sec}$, exponential-

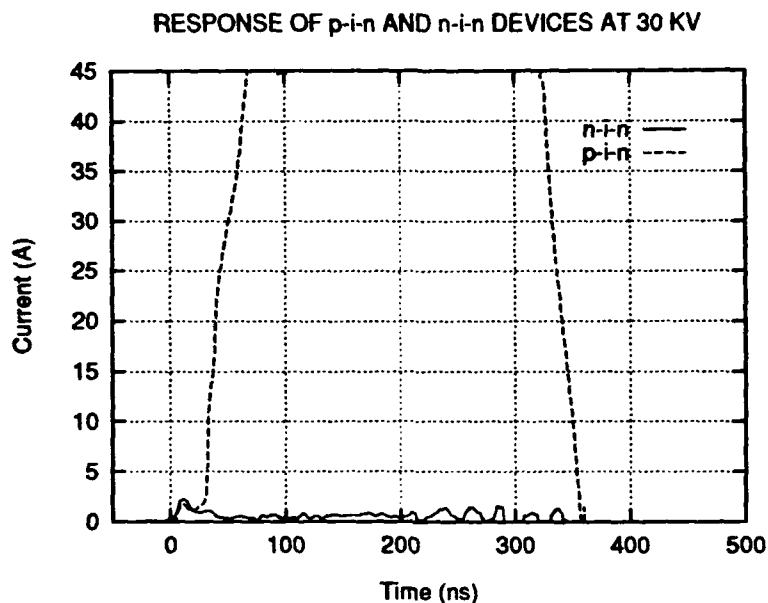


Figure 2-9. I-V curves for a) p^+i-n^+ and b) n^+i-n^+ devices. The dimensions of the p^+i-n^+ and n^+i-n^+ devices were about $10 \times 7 \times 2.5$ mm, and $10 \times 8 \times 2.5$ mm, respectively. The experimental conditions for both curves were the same: 30 kV, 290 ns rectangular pulse, vacuum ambient ($<10^{-6}$ Torr).

decay pulses of magnitude up to 40 kV. This is a significant improvement over either a single-piece or a laminated device. Flashover did occur when the voltage was increased to 50 kV, and a single breakdown event produced considerable damage to the sample. At 50 kV, the delay to the onset of breakdown was 50–100 ns for a device which had not broken down previously.

2.4 A Device for Making Pulsed I-V Measurements in the 0-800 V Range

We routinely measure the low-voltage (0-800 V) I-V curves for the devices we make to check the quality of the contacts and doping. For voltages above about 100 V, voltage pulses must be used to avoid sample heating. For this purpose we designed and built a computer-controlled circuit which delivers pulses of variable duration and magnitude up to about 800 V, and measures the current during the voltage pulse. Fig. 2-12 shows a schematic diagram of the circuit. Briefly, a D/A converter in a 386-based computer provides a voltage proportional to the desired pulse voltage. This voltage is used to control a switching type DC-DC converter which can provide voltages up to about 800 V. T-channel FET's are used as switches to connect and disconnect the output of the converter to the sample under test. A/D converters are used to read the actual voltage applied to the sample and the voltage across a current-viewing resistor in series with the sample. Finally, software in the computer controls the timing, collects the data, and plots the results.

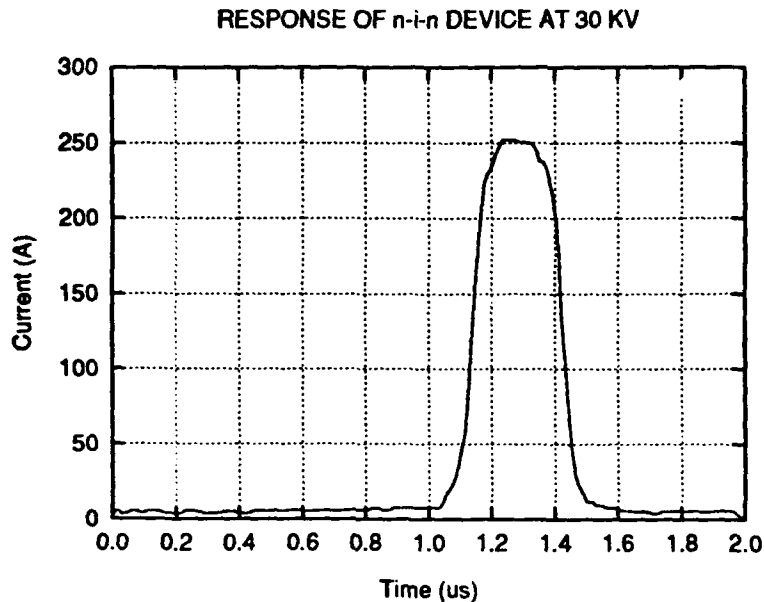


Figure 2-10. Plot of current vs time for a $n^+ - i - n^+$ sample. The sample dimensions were $9 \times 8 \times 2.5$ mm, and the voltage was applied across the 10 mm dimension. The peak voltage was 30 kV. The risetime was 20 ns, and the voltage decayed with a time constant of $5 \mu\text{sec}$.

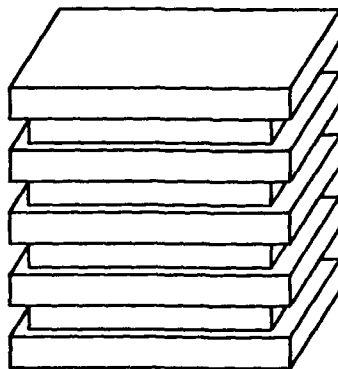


Figure 2-11. Schematic drawing of the grooved device discussed in the text. The overall device dimensions were $10 \times 8 \times 2.5$ mm, and the grooves were 1 mm wide and 0.5 mm deep. Masking for etching the grooves was done manually, and the grooves in the actual device were somewhat more irregular than indicated in the figure.

2.5 Photo-current Imaging

From our previous results, it is clear that changing the surface properties of our silicon samples can have substantial effects on the flashover characteristics of the samples. For example, we find that there is an aging effect whereby samples which have undergone

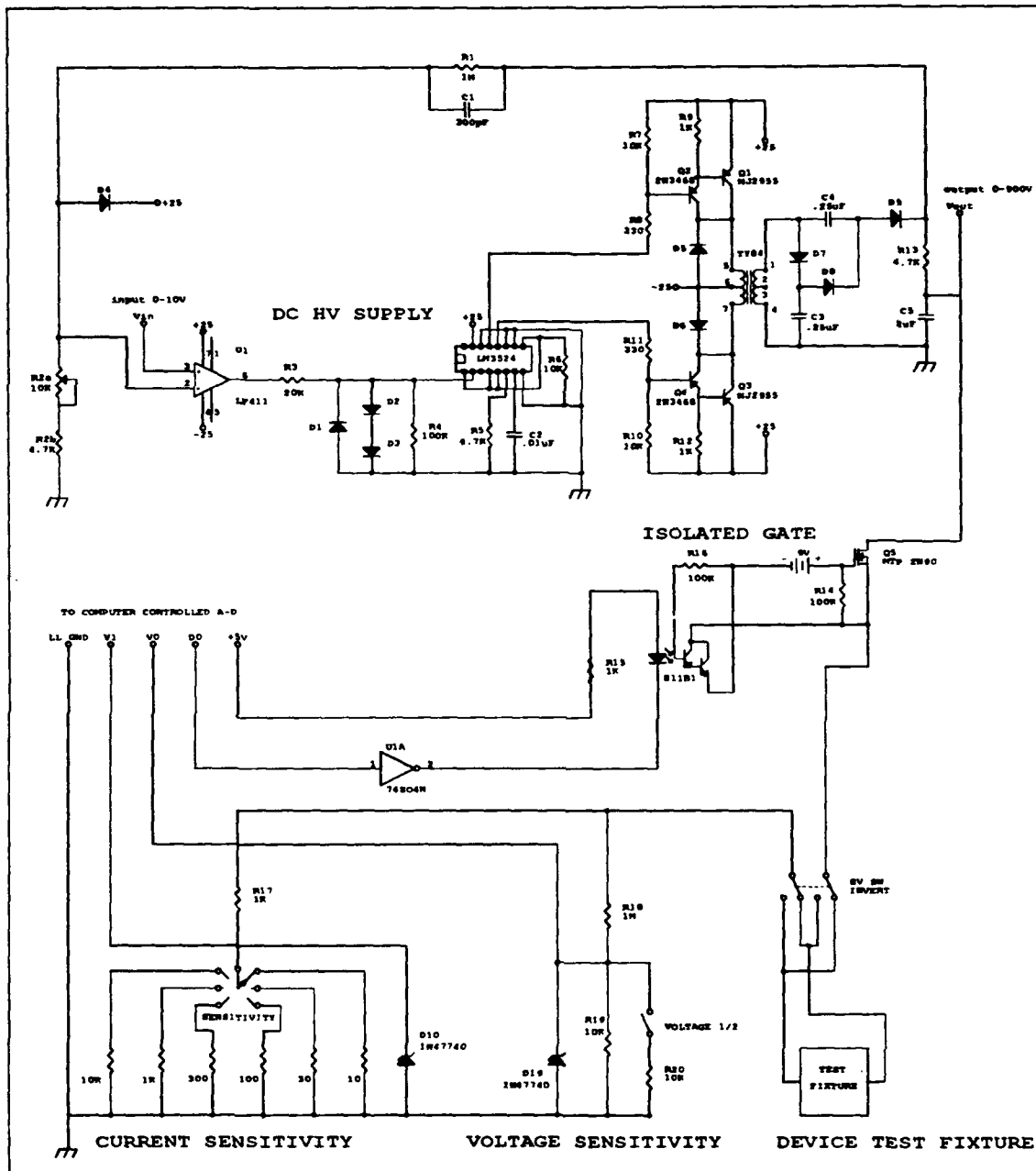


Figure 2-12. Schematic diagram of the voltage pulser built to measure I-V curves of silicon samples for voltages up to 800 V.

many (typically >200) flashover events do not flashover as readily as do new samples. Presumably that difference is due to surface damage induced by the flashovers. This conclusion is consistent with our qualitative observation that flashovers on relatively new samples occur on different areas of the surface each time. As another example, the

flashover inhibition effect of weak illumination discussed in section 2.1.3.1 presumably works by modifying temporarily the properties of the surface. Still another example is the reported effect of various environments on the flashover of silicon and gallium arsenide devices. Hold-off voltages differing by more than a factor of two are reported for otherwise similar devices immersed in different liquids and gases.^{[5]c [6]} Since the processes responsible for initiating flashover must be occurring inside the semiconductor, these differences must be due to ambient-induced modifications of the properties of the surface.

In order to investigate these phenomena, we constructed a facility for mapping the surface of our silicon samples using the photo-current induced by the focussed beam from a He-Ne laser. The sample under test was mounted on a computer-controlled translator table capable of motion in two dimensions, and a low bias voltage (about 10 V) was applied across it in the forward direction. The chopped beam from a He-Ne laser was attenuated and focussed to a point on the sample surface and the resulting photo-current monitored using a lock-in amplifier, and stored in the computer. The computer was programmed so that the entire surface of the sample was scanned and the resulting photo-current saved. At the end of a run, the result could be read out or plotted. Fig. 2-13 shows atypical results obtained from a p^+i-n^+ silicon sample with light surface damage.

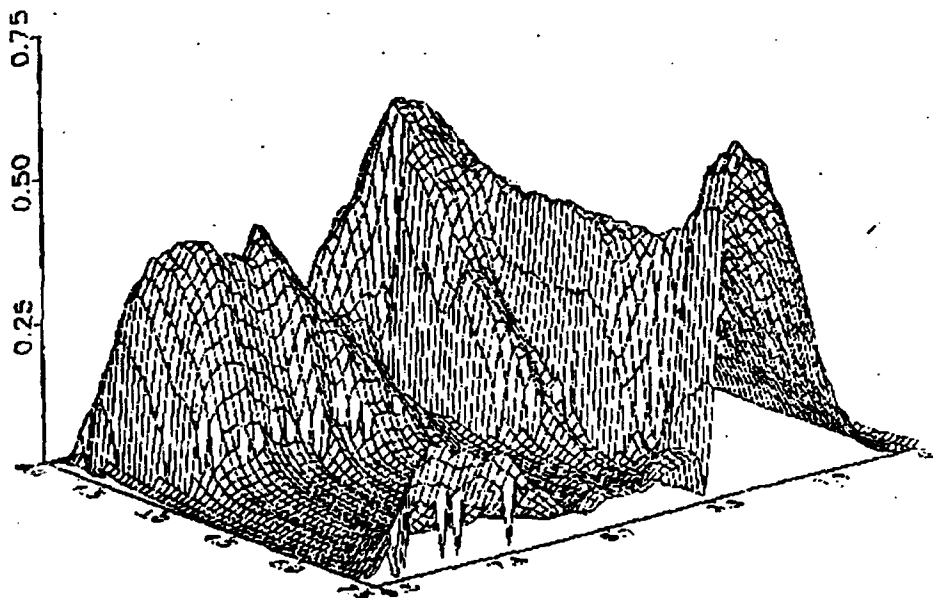


Figure 2-13. Surface plot showing the photoresponse produced by an atypical p^+i-n^+ sample. The scales on the two spatial axes are in mm from one corner of the sample. Voltage was applied along the long dimension. The z -axis is the photocurrent expressed in relative units.

More typical results displayed less structure and weaker signal levels.

The results of these experiments have proven difficult to analyze. The photocurrent at any point should be proportional to the longitudinal electric field, the number

of photo-carriers produced, and the lifetime of these carriers. We had hoped that the latter two factors would be nearly constant over the the surface of the sample so that our photo-current measurements would yield results proportional to the longitudinal component of the electric field. If this is the case then, since the voltage across the sample is fixed, the integral of the photo-current readings along any path connecting one electrode to the other should be about the same and proportional to this voltage. As is evident in Fig. 2-13, this is clearly not the case. Similar difficulties were encountered with other, more typical, data sets. Presumably these variations in photo-current reflect variations in either the production of photo-carriers or in the trapping of them across the surface. That information would be interesting, but it is difficult to deconvolute the effects of variations in the individual factors.

Although these data do not provide direct information about the electric field in our samples as we had hoped, they do show clearly that relatively minor modifications of the surface can have significant effects on carrier dynamics. We saw significant variations in photo-current across the surfaces of nominally undamaged samples, and the magnitude of the photo-response varied considerably between samples which had been treated similarly.

2.6 Mid-Voltage Transient Current Measurements

In high-voltage current vs. time traces obtained in experiments in which the sample did not flashover (such as the solid trace in Fig. 2-8) we observed a slow rise in current from the roughly 3 A value at the start of the voltage pulse to about 10 A at the end of the -290 ns pulse. We initially believed this current rise was due to sample surface heating, and sought to investigate it more closely. To do so, we applied to our samples variable length voltage pulses of magnitude such that flashover did not occur, and monitored the current. Fig. 2-14 shows a typical result. After the initial rapid current rise at the pulse leading edge, the current continues to rise at a much slower rate and then levels off after about 4 μ s at a value about twice the initial current.

If this slower rise were due to a heating effect it should continue to rise, rather than levelling off. We believe that this behavior is a result of the space-charge-limited nature of current flow in our samples under these conditions, and of the fact that this current flow is decidedly not one-dimensional. At the start of the voltage pulse, carriers are injected into the semiconductor from each contact, producing a space-charge near each contact which limits further injection. As these carriers drift away from the contact in the applied field, the field at the contact from the carriers decreases and more charge is injected. We believe that this increased charge is responsible for the current increase we observe. The effect would not be present in a sample for which a one-dimensional model is accurate because the field from an infinite sheet of charge does not decrease with distance.

In our samples, the width of the charge sheet is limited by the sample thickness to about 2 mm. The field at the contact from this sheet of shielding charge would be expected to decrease when the sheet had drifted a distance away of the order of the sheet width (2 mm in our case). More charge would then be injected to reduce the field at the

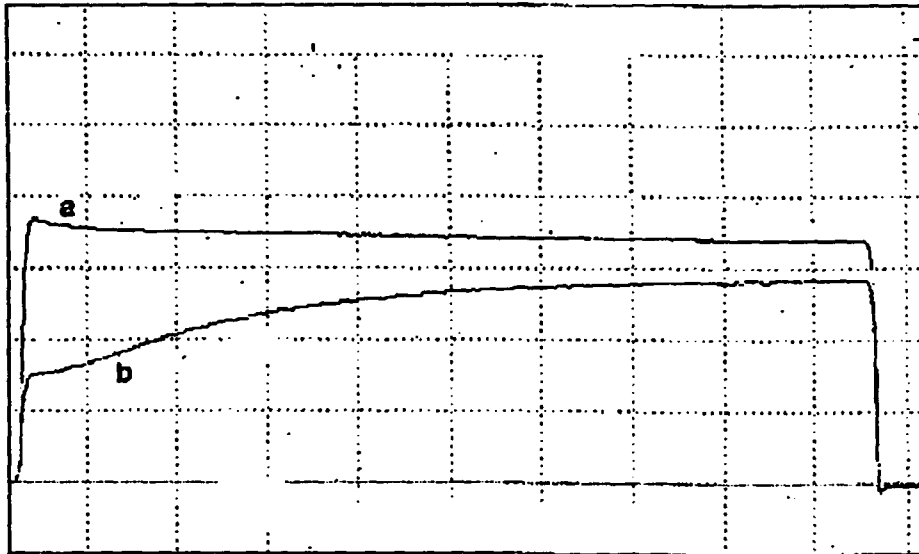


Figure 2-14. Oscilloscope traces showing sample voltage (a) and current (b) in a p^+i-n^+ sample when subject to a 1700 V pulse. The scale for the voltage pulse is 500 V/div., and that for the current trace is 143 mA/div.

contact to nearly zero. Assuming the carrier mobility to be 1000 V-cm/sec, and a field of 1.5 kV/cm, the carrier velocity would be about 1.5×10^6 cm/sec. At this speed, about 100 ns would be required for the carriers to drift 2 mm, and this would be the expected time scale for the current to increase initially. About 700 ns would be required for the carriers to drift the length of the sample. Ignoring carrier injection from the opposite electrode, one would expect a roughly steady-state flow to have been achieved by this point. The current trace in Fig. 2-14 shows that a steady state flow is reached, but after a somewhat longer time of about 4 μ s, rather than 700 ns. The sample was a p^+i-n^+ structure, so injection from the opposite contact cannot be ignored. Double injection effects, coupled with the lower mobility of holes in silicon may be responsible for the time differences.

2.7 Photo-response to a Weak Probe Pulse

We have carried out a set of experiments intended to help us understand current transport in our samples. In these experiments a selected region of a biased sample was illuminated with a weak pulse of light, and the resulting current response monitored. We have used both low (~ 20 V) and moderate (~ 1500 V) bias, and have measured the time-dependent current response for several spatial shapes and locations of the illumination. One of the goals of these experiments was to investigate further the phenomenon discussed in the previous section in which currents thought to be space-charge limited increased with time. Another goal was to try to learn more about the spatial mapping experiments discussed in Section 2.1.5, and about why the results are so inconsistent with our original supposition that the photo-current would be a measure of the electric field.

Several photo-current pulses obtained with a 15 ns, 40 μ J pulse of 532 nm illumina-

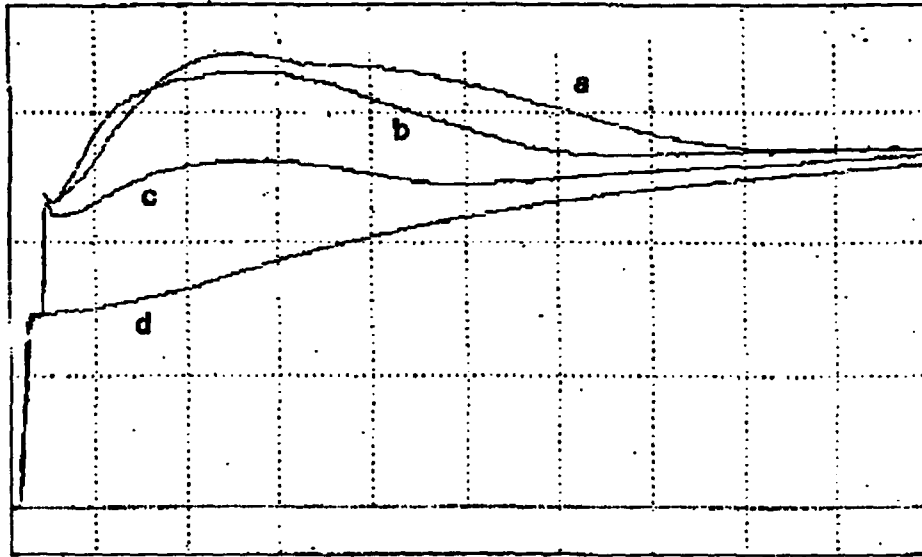


Figure 2-15. Oscilloscope traces showing the sample current for the same sample as that used for the data in Fig. 2-14. The traces marked (a), (b), and (c) were obtained by illuminating the sample with a 15 ns, 40 μ J pulse of 532 nm light. Also shown, and marked as (d), is the curve obtained without illumination. For the curves obtained with sample illumination, the illuminated region was a rectangular region which covered the entire width of the sample, and extended 4 mm along the sample axis. For the curve marked (a), the region was at the anode end of the sample, for (b) it was in the middle, and for (c) it was at the cathode end.

tion from a Nd:YAG laser are shown in Fig. 2-15. Also shown in the figure is the current observed without illumination. For all but this last curve, the sample was illuminated with a rectangular region which covered the full width of the sample, and extended 5 mm along the axis of the sample. The separate curves were obtained with differing positions of the illuminated region on the sample surface. The sample was pulse charged to 1700 V. The arrival of the optical pulse is clearly evident as a sharp current rise. Even though the optical intensity returns to zero within ~ 15 ns, the current continues to rise for about 1μ s, before decaying with a $1-2 \mu$ s time constant. In this case the optical pulse produced sufficient free carriers that they formed a plasma capable of shielding the interior of the plasma region from the applied bias field. The behavior of the resulting space-charge limited current from this plasma is similar to that measured in the previous section, and thought to be the result of space-charge limited carrier injection at the contacts.

Because of the shielding, after a very short transient in which the shielding sheaths were set up, only those carriers in the shielding sheaths contributed substantially to the current. As these carriers move away from the localized plasma, they become less and less effective in canceling the applied field within it, and new carriers must be added to the sheath. With the contribution of these carriers, the current rises. As the process

continues, carriers are lost due to recombination and perhaps to transport out of the sample. Eventually, this reduction in total carrier number causes the current to decrease. The time scale for carrier reduction due to recombination would be expected to be of the order of a minority carrier lifetime, $2-5\mu\text{s}$ in our samples, consistent with the position of the peak in the current trace of Fig. 2-15.

In order to verify that the currents we saw in these experiments were in fact limited by space-charge, we carried out experiments in which the spatial shape or the initial density of the photo-plasma was varied. For a given applied field, the charge required in the plasma sheath to shield the plasma interior depends on the cross-sectional area of the plasma normal to the field direction. The larger the area, the larger the charge required. Thus if the photo-currents were space-charge limited, then we should see a relation between this normal cross-sectional area and the photo-current. The cross sectional area could be varied in the direction parallel to the surface by varying the shape of the illuminating beam, and in the direction normal to the surface by changing the illumination wavelength (due to changing absorption depth). Although there were a few complications, the behavior we observed was consistent with a space-charge-limited model of current flow.

Another check on the space-charge-limited nature of the currents involves varying the intensity of the optical beam which creates the carriers. For a sufficiently weak beam, the density of carriers becomes small enough that the "plasma" is unable to shield itself effectively from the applied field. Below the threshold for shielding, the magnitude of the photo-current pulse is expected to vary linearly with optical intensity because all the photo-carriers contribute equally to the current, but above the threshold the magnitude of the photo-current pulse would be expected to vary sub-linearly with optical intensity because only a fraction of the carriers produced contribute to the current. Fig. 2-16 shows the results of such an experiment. For pulse energies below about $1\mu\text{J}$ the magnitude of the photo-current jump depends linearly on the pulse energy, but then curves sharply away from the extrapolated straight line. This saturation effect is that expected from the formation of a photo-plasma.

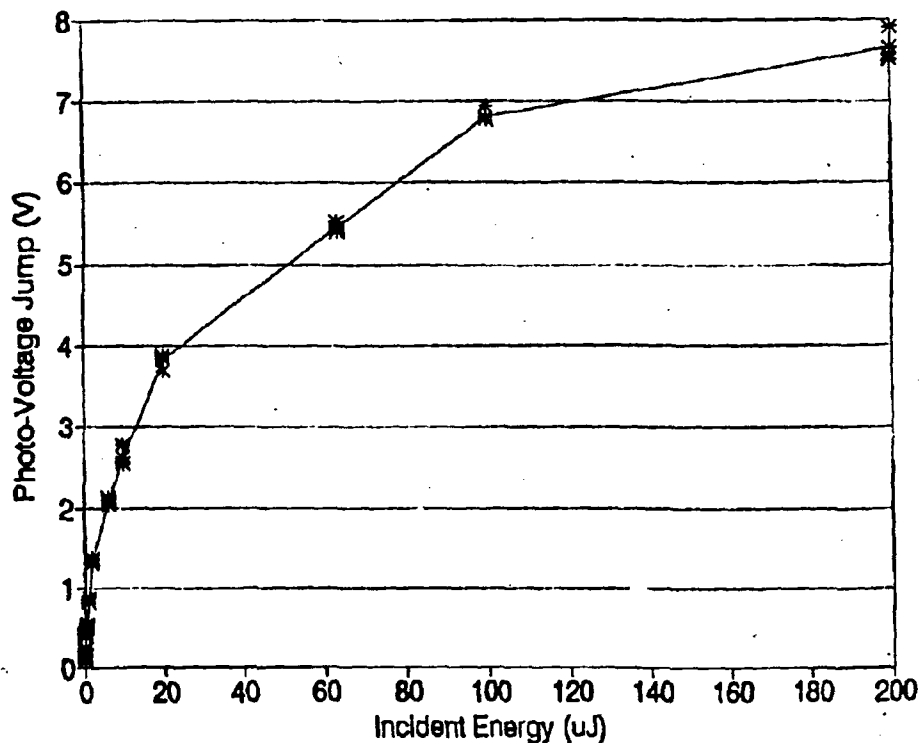


Figure 2-16. Plot showing the dependence of the magnitude of the current pulse associated with an optical illumination pulse on the energy of the optical pulse.

2.8 Double Injection Effects

In the course of characterizing our sample contacts, we obtained an I-V curve for a p^+i-n^+ device with a ~ 2 mm long, ~ 15 $k\Omega\text{-cm}$ intrinsic region. Fig. 2-17 shows the curve as obtained with a semiconductor parameter analyzer operated in the controlled-current mode. In the forward direction, device current increases supra-linearly with voltage until a threshold is reached, whereupon the voltage falls abruptly with increasing current in several sharp steps. After a region of negative differential resistance, the resistance again becomes positive but small. This behavior was quite reproducible, and the voltage threshold was very sharp. Although there were some changes due to sample heating, we observed the same behavior using a D.C. power supply and an ammeter in place of the parameter analyzer.

We believe this effect to be due to double injection. The effect was not seen in singly injecting n^+i-n^+ devices of otherwise similar construction. To further investigate this hypothesis, we measured the time dependence of the device current using a pulsed voltage source. Fig. 2-18 shows current oscillograms obtained using pulse voltages of 23.5 and 24.0 V. These voltages are just below and just above, respectively, the threshold voltage for double injection currents. In the figure, we see that the above-threshold current initially rises to a value similar to the current with the below-threshold voltage.

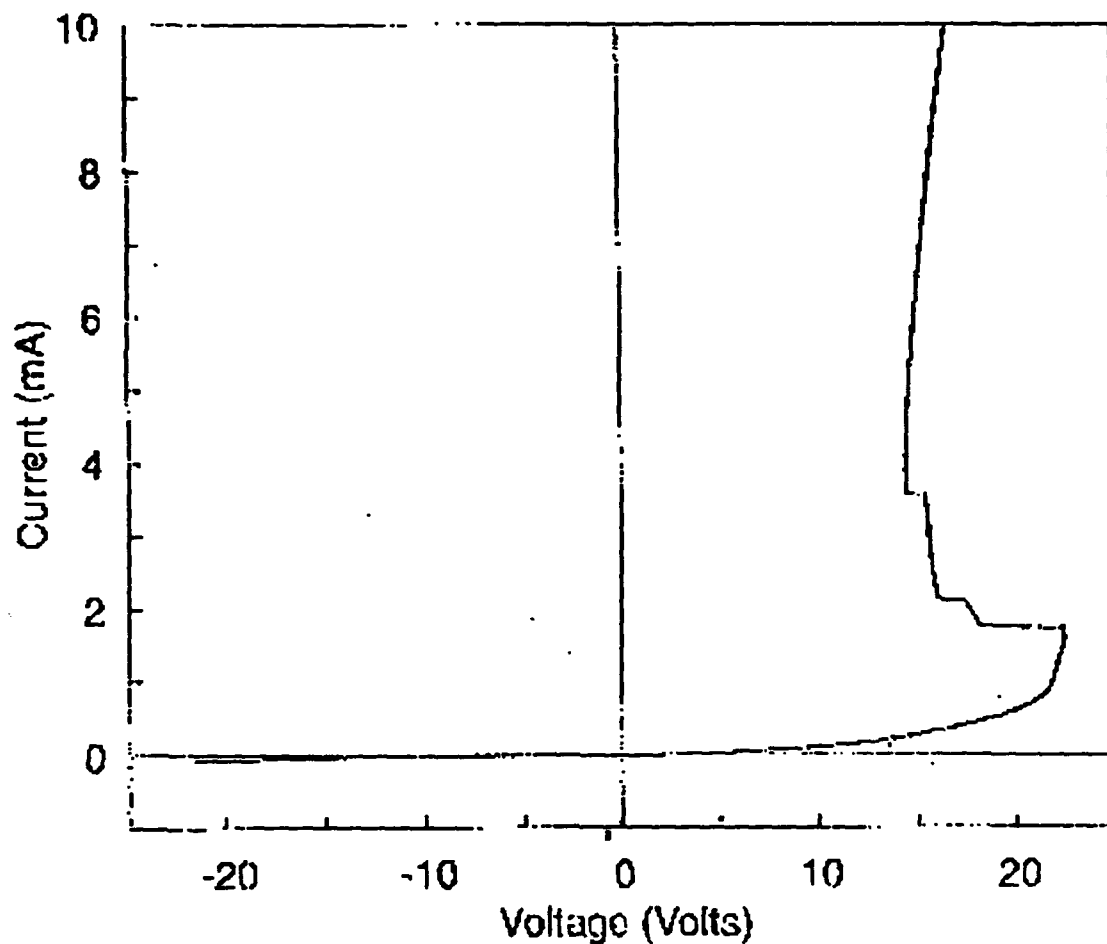


Figure 2-17. I-V curve for an 0.2 cm long $p^+ - i - n^+$ device displaying effects of double injection.

Above threshold, the current does not stabilize, however, and increases with a time, slowly at first, and then more rapidly. For double injection to occur, a delay time of at least several carrier transit times is required because the effect involves the cancellation of space charge near the cathode by holes injected at the anode. For this applied voltage, about $18 \mu\text{sec}$ is required for a hole to traverse the 2 mm length of the device. The "turn-on" delay for the 24.0 V curve in the figure is therefore about 40 transit times. Farther above threshold, the delay time decreased substantially to $100 - 200 \mu\text{sec}$. Similar temporal behavior has been observed with high resistivity $p^+ - i - n^+$ silicon devices with a 3 mm long intrinsic region by Baron, Marsh, and Mayer.^[7] They did not observe a negative resistance region, however. Negative resistance due to double injection effects in high voltage GaAs switches has been predicted theoretically by Brinkmann, Schoenbach, and Stoudt,^[8] and more generally in semiconductors and insulators by many authors.^[9]

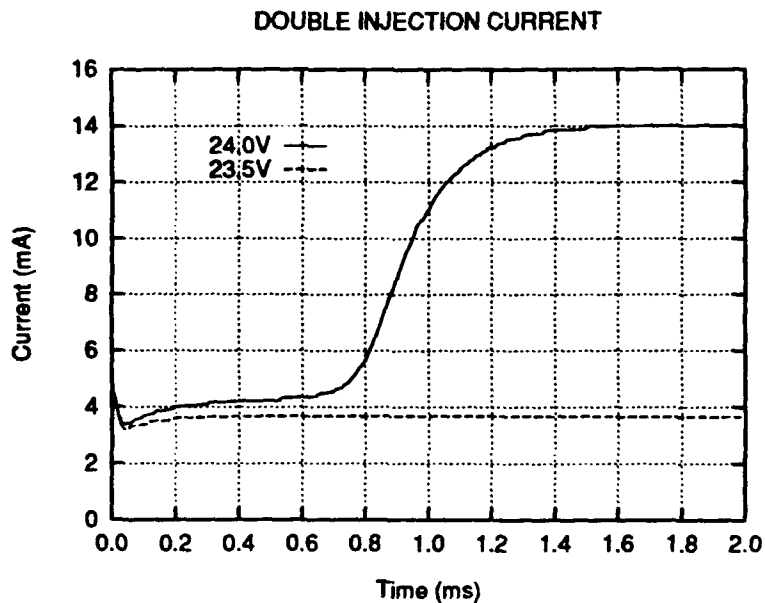


Figure 2-18. Plot of device current vs time for the device used to obtain the data shown in Fig. 2-17 for two different applied voltages. The dashed curve shows data for an applied voltage just below the threshold for double injection, and the solid curve is for an applied voltage 0.5 V higher.

2.9 Qualitative Model of Flashover Initiation

2.9.1 Previous Work in the Field

The problem of surface flashover of semiconductors such as silicon and germanium has been known for more than 30 years.^[10] In a reverse-biased junction the applied voltage appears across a narrow depletion region centered at the junction. In favorable cases the maximum hold-off voltage of these devices was limited by bulk avalanche multiplication inside the semiconductor, but more commonly flashover occurred at the surface at voltages lower than that required for bulk breakdown. It was found that the surface flashover voltage could be increased by coating the semiconductor surface with a high dielectric constant material such as castor oil.^[11] Later, the problem was overcome by beveling the edges of the device. This technique increases the surface distance between the edges of the depletion region, thereby reducing the tangential field. By using very acute beveling angles it was possible to increase the surface length to the point that the hold-off voltage of the device was limited by bulk avalanche breakdown at the junction rather than by surface processes.^[12-15]

Because of the requirement that the hold-off voltage must be dropped across a narrow depletion region, junction devices are generally limited to maximum voltages of 1-10 kV, and the beveling solution has proven adequate for these devices. With the renewed interest in bulk devices such as photoconductors for high voltage applications, the problem has reappeared. In these devices the voltage appears across the entire length of the

semiconductor, rather than across a narrow depletion region, and edge beveling is not a suitable solution to the problem of surface flashover. If the bulk devices are to achieve their potential in high voltage applications, other solutions must be found.

Several models of insulator flashover have appeared, most of which are based on some type of surface charging phenomenon.^[16] In all of the models of surface flashover of insulators the actual breakdown occurs in the surrounding ambient, not in the insulator. The insulator may act to produce an enhanced electric field through surface charging or some other mechanism, but the process (e.g. avalanching) leading to breakdown occurs in the ambient. We have shown clearly that at least for $p^+ - i - n^+$ silicon structures, the breakdown occurs inside the semiconductor, rather than outside it, as assumed in these models. These models are, therefore, inadequate to explain surface flashover of semiconductors.

2.9.2 Our Model for the Surface Flashover Mechanism

We have developed a model in which the flashover initiation process occurs on the semiconductor side of the interface, rather than in the ambient.^[17] The model is based on band bending at semiconductor surfaces subjected to normal electric fields. We propose that the resulting surface conductivity causes surface heating and/or potential redistribution which then lead to flashover. The predictions of the model are dependent on the magnitude of the perpendicular electric field component at the semiconductor surface. This field depends on the geometry, on surface charging of the semiconductor, and on the carrier dynamics inside the semiconductor. The dynamics of the surface heating and potential redistribution processes are complicated, and we treat them very simply.

Band bending and the consequent modification of the surface conductivity of a semiconductor upon application of a perpendicular electric field is a well-known phenomenon on which MOSFET transistors and charge transfer devices are based.^[18] There is insufficient information from experiments to determine whether the flashover observed on semiconductor surfaces of $n^+ - i - n^+$ structures results from this band bending mechanism or from some other mechanism with a lower voltage threshold. For $p^+ - i - n^+$ structures, it appears that the flashover we observe occurs too rapidly to be explained solely by this mechanism, and that some other mechanism must contribute. The phenomenon of surface conductivity modification due to band bending is sufficiently well-established, however, that the validity of the mechanism on which the model is based is not in question.

Consider a slab of semiconductor material in an electric field with normal component E_{\perp} . The normal field may be caused by charging of insulating surface films, or by geometric effects. In steady state, this field results in a surface charge density $\sigma = \epsilon_0 E_{\perp}$ contained in a layer of thickness given roughly by the Debye length, L_D ,

$$L_D = \left[\frac{\epsilon k T}{q^2 n} \right]^{1/2} \quad (2-1)$$

where n is the volume carrier density (either holes or electron, depending on the sign of the normal field), ϵ is the dielectric permittivity of the semiconductor, k is Boltzmann's

constant, T the temperature, and q the charge on an electron. Setting $n = \sigma/qL_D$, and solving gives

$$n = \frac{\epsilon_0}{\epsilon} \frac{\epsilon_0}{kT} E_{\perp}^2 \quad (2-2)$$

For example, in intrinsic silicon a normal field of 100 kV/cm would result in a surface carrier density of about $2 \times 10^{16} \text{ cm}^{-3}$, distributed over a layer of thickness 30 nm. More accurate calculations give a carrier density of $1 \times 10^{16} \text{ cm}^{-3}$, and a thickness of about 40 nm.

In the presence of a longitudinal field, these carriers are swept toward one contact. In the absence of trapping, there is a balance between carrier loss through capture at one contact, carrier injection at the other contact, and carrier generation in the unshielded volume of the semiconductor. Surface flashover may occur due to ohmic heating of the surface, or field enhancement resulting from potential redistribution along the surface caused by non-uniform surface conductivity or inefficient carrier injection at an contact. In practice, both mechanisms probably play a role.

To obtain a rough estimate of the time required for the surface discharge to develop, we assume that flashover results solely from ohmic heating of the semiconductor surface due to carrier drift under the influence of the longitudinal field. For simplicity we assume uniform carrier density and electric field everywhere on the surface. Since the development of non-uniformities will lead to faster local heating, we expect the flashover time we estimate to be longer than actually observed. As the temperature rises, thermal excitation of carriers increases, increasing exponentially the free carrier density and the heating rate. The sequence of events after this point is complicated, with a number of processes potentially playing a role. We avoid these problems by assuming that the heating rate remains constant, and estimating the flashover time to be the time for the surface temperature to increase by some arbitrarily-chosen ΔT at this rate. Neglecting heat loss, the surface temperature increases at the rate

$$\frac{dT}{dt} = \frac{nq\mu E_z^2}{c_p \rho_m} \quad (2-3)$$

Using Eq. (2-2) the flashover time is,

$$t_{flashover} = \frac{\epsilon}{\epsilon_0} \frac{kT}{q\mu} \frac{c_p \rho_m}{\epsilon_0 E_{\perp}^2 E_z^2} \Delta T \quad (2-4)$$

where μ is the carrier mobility, c_p is the specific heat, ρ_m the mass density of the semiconductor, and E_z is the field tangential to the surface. Using values appropriate to silicon, $E_z = 30 \text{ kV/cm}$, and taking $\Delta T = 400 \text{ }^\circ\text{C}$, we estimate flashover to occur in about $1.6 \mu\text{s}$ for $E_{\perp} = 50 \text{ kV/cm}$, consistent with flashover times normally found for $n^+ \text{-i-} n^+$ structures. Such a surface field can easily be produced by charging of oxidized silicon surfaces. The choice of $\Delta T = 400 \text{ }^\circ\text{C}$ is quite arbitrary, but it should provide a reasonable (factor of two) estimate of $\tau_{flashover}$. We find experimentally that $p^+ \text{-i-} n^+$ structures

breakdown in a time about 100 times shorter than this value. Our model would require an unreasonably large transverse field of about 500 MV/cm to explain such a short time.

2.9.3 Discussion of the Model

The estimates in the previous section show that the band bending mechanism can explain the phenomenon of surface flashover of n^+i-n^+ structures using a reasonable value (~ 50 kV/cm) for the normal surface field. There is insufficient empirical information to determine whether the flashover observed in practice for these structures is the result of this mechanism, or of some other unknown mechanism. Some other mechanism must contribute to breakdown for p^+i-n^+ structures. In any case, the band bending mechanism should be operative, and should be considered in designing high voltage solid state switches. For example, a strip line geometry is often used in very fast photoconductive switches. For high voltage switches designed with this geometry, the surface field could easily reach values for which the mechanism limits the performance of the switch.

The model discussed above apparently requires normal surface fields of the order of 100 kV/cm to produce flashover in times seen experimentally. For experiments carried out with uniform field geometry electrodes, and in a highly insulating ambient such as high vacuum or insulating gas, charging of the native oxide surface is probably required to produce such fields. There is some evidence supporting, or at least consistent with, the importance of surface charging. The occurrence of flashover is generally found to be erratic in that a sample may flashover on the n^{th} pulse after withstanding $n - 1$ pulses of the same voltage. This behavior is consistent with the development of a persistent charge on the oxide surface.

The calculations discussed in the previous section are based on a number of approximations. Most important are the assumption of surface uniformity, and the much oversimplified model of the flashover process we used. Based upon the observation of glow-to-arc transitions and of streamer formation in gas breakdown, we expect that the formation of domains of higher conductivity is likely to play an important role in the flashover process. These effects are not considered in our estimate. Further, Donaldson^[19] reports the measurement of the electric field magnitude above a stressed silicon sample. He found that the field was maximum at the ends of the sample, implying that contact effects may be important. The effects were ignored in our estimate, and the assumption of uniformity precludes consideration of such effects.

The calculation of the carrier density at the surface, and the resulting rate of temperature rise can be done more accurately. We have carried out such calculations, but do not discuss them here because they require numerical solution of transcendental equations and are not particularly illuminating. The more accurate calculations result in carrier densities about half and, therefore, flashover times about twice those predicted by our approximation. We have also ignored effects of the surface or of temperature on carrier mobility, and heat conduction out of the surface region. These effects could be included in a numerical calculation without a great deal of added difficulty.

From our experimental results, it is clear that current in a surface flashover event flows primarily close to the surface, and that current filamentation plays an important role

at least in the later stages of a flashover event. Although many of the details remain to be worked out, it is not difficult to see how heating and trap filling could lead to breakdown, given as an initial condition a current sheet at or near the surface of sufficient density.

The model does not consider contact effects, so it does not explain the observed difference between flashover with p^+i-n^+ and n^+i-n^+ structures. This observation, coupled with the difficulty explaining the very fast breakdown in p^+i-n^+ structures and the results of our studies described earlier of space-charge-limited current flow, lead us to conclude that there is at least one additional, significant process involved with the breakdown of p^+i-n^+ structures. One mechanism which is missing from the model is the effect of the two-dimensional nature of the space-charge-limited current flow near injecting electrodes. When voltage is applied to the semiconductor carriers are injected from one or both contacts. The space-charge from these injected carriers limits further injection by producing a field at the contact which is roughly equal in magnitude to the applied field, but opposite in sign. These effects have been thoroughly studied for the one-dimensional case, but because of the geometry of our sample, our case is decidedly at least two-dimensional. Besides having a longitudinal component, the space-charge field also has a transverse component of comparable magnitude which causes charge to move to the surface. This build up of surface charge occurs on a time scale given by the dielectric relaxation time of the semi-insulating semiconductor material, (about 1 ns for our samples). This surface charge is confined to the near surface region by the transverse fields, but it is free to move longitudinally, and is a likely candidate for the initial source of surface current density responsible for initiating flashover.

REFERENCES

1. S.K. Ghandi, *The Theory and Practice of Microelectronics*, (Wiley, New York, 1968).
2. S.M. Sze, *Semiconductor Devices Physics and Technology*, (Wiley, New York 1985), pp. 92-96.
3. F.E. Peterkin, P.F. Williams, B.J. Hankla, L.L. Buresh, S.A. Woodward, "Inhibition of Surface-Related electrical Breakdown of long $p^+ - i - n^+$ Silicon Structures," *Appl. Phys. Lett.* **62**, 2236-39 (1993).
4. F.E. Peterkin, T. Ridolfi, L.L. buresh, B.J. Hankla, D.K. Scott, P.F. Williams, W.C. Nunnally, and B.L. Thomas, "Surface Flashover of Silicon," *IEEE Trans. Elect. Devices*, **37**, 2459-65 (1990).
5. G.M. Loubriel, M.W. O'Malley, and F.J. Zutavern, "Toward Pulsed Power Uses for Photoconductive Semiconductor Switches: Closing Switches," in *Digest of Technical Papers, Sixth IEEE Pulsed Power Conference*, edited by B.H. Bernstein and P.J. Turchi (IEEE, New York, 1987), pp. 145-48.
6. M. Pocha, presentation at the Optically and Electron-Beam Controlled Semiconductor Switches Workshop, Norfolk, VA, 1988; and W. Hofer and R. Druce, private communication.
7. R. Baron, O.J. Marsh, and J.W. Mayer, "Transient Response of Double Injection in a Semiconductor of Finite Cross Section, *J. Appl. Phys.* **37**, 2614-2626 (1965).
8. R.P. Brinkmann, K.H. Schoenbach, and D.C. Stoudt, "The Current-Voltage Characteristics of Semi-Insulating Gallium Arsenide," Old Dominion University Physical Electronic Research Institute report, Publication Series No. 105-6/90.
9. See for example M.A. Lampert and P. Mark, *Current Injection in Solids*, (Academic, New York, 1970).
10. H.S. Veloric, and M.B. Prince, "High-Voltage Conductivity-Modulated Silicon Rectifier," *Bell Syst. Tech. J.*, pp. 975-1004 (1957).
11. S.L. Miller, *Phys. Rev.* **99**, 1234 (1955).
12. O.M. Clark, "Voltage Breakdown of Silicon Rectifiers as Influenced by Surface Angle," *J. Electrochem. Soc.* **107**, p. 269C (1960).
13. R.L. Davies and F.E. Gentry, "Control of Electric Field at the Surface of P-N Junctions," *IEEE Trans. Electron Devices ED-11*, pp. 313-323 (1964).
14. J. Cornu, "Field Distribution Near the Surface of Beveled P-N Junctions in High-Voltage Devices," *IEEE Trans. Electron Devices ED-20*, pp. 347-352 (1973).
15. J. Cornu, S. Schweitzer, and O. Kuhn, "Double Positive Beveling: A Better Edge Contour for High-Voltage Devices," *IEEE Trans. Electron Devices ED-21*, pp. 181-184 (1974).

16. See for example T.S. Sudarshan and R.A. Dougal, "Mechanisms of Surface Flashover Along Solid Dielectrics in Compressed Gases: A Review," *IEEE Trans. Elect. Insulation EI-21*, pp. 727-746 (1986).
17. P.F. Williams and F.E. Peterkin, "A Mechanism for Surface Flashover of Semiconductors, *Digest of Technical Papers, Seventh IEEE Pulsed Power Conference*," edited by B.H. Bernstein and J.P. Shannon, (IEEE, New York, 1989), pp. 890-92.
18. C.G.B. Garrett, W.H. Brattain, "Physical Theory of Semiconductor Surfaces," *Phys. Rev.* 99, pp. 376-387 (1955).
19. "Optical Probes for the Characterization of Surface Breakdown," W.R. Donaldson, S.P.I.E. Paper No. 87124 (1987).

3. WORK AT THE UNIVERSITY OF TEXAS AT ARLINGTON

The work carried out at UTA is described in detail in the following pages.

4. CUMULATIVE LIST OF PUBLICATIONS

1. "A Mechanism for Surface Flashover of Semiconductors," P.F. Williams and F.E. Peterkin, in *Digest of Technical Papers, 7th Pulsed Power Conference*, B.H. Bernstein and J.P. Shannon eds., pp. 890-92 (1989).
2. "Recent Developments in the Investigation of Surface Flashover on Silicon Photoconductive Power Switches," B.L. Thomas and W.C. Nunnally, in *digest of Technical Papers, 7th Pulsed Power Conference*, B.H. Bernstein and J.P. Shannon eds., pp. 893-96 (1989).
3. "Surface Flashover in Silicon Photoconductive Power Switches," B.L. Thomas, Ph.D. Dissertation, University of Texas at Arlington (1989).
4. "Surface Flashover of Silicon," F.E. Peterkin, T. Ridolfi, L.L. Buresh, B.J. Hankla, D.K. Scott, P.F. Williams, W.C. Nunnally, and B.L. Thomas, *IEEE Trans. on Electron Devices* **12**, 2459-65 (1990).
5. "Surface Flashover of Silicon, P.F. Williams," F.E. Peterkin, T. Ridolfi, L.L. Buresh, and B.J. Hankla, *Optically Activated Switching*, S.P.I.E. Vol. 1378 (S.P.I.E., Bellingham, WA, 1991), pp. 217-225.
6. "Surface Field Measurement of Photoconductive Power Switches," H.P. Sardesai, W.C. Nunnally, and P.F. Williams, *Optically Activated Switching*, S.P.I.E. Vol. 1378 (S.P.I.E., Bellingham, WA, 1991), pp. 237-248.
7. "Surface Flashover of Silicon," F.E. Peterkin, P.F. Williams, T. Ridolfi, B.J. Hankla, and L.L. Buresh, *Digest of Tech. Papers, Eighth IEEE Int. Pulsed Power Conf.*, K. Prestwich and R. White eds., (IEEE, New York, 1991), pp. 118-121.
8. "Optical Measurements of Surface Electric Fields on Silicon Photoconductive Power Switches," H.P. Sardesai, W.C. Nunnally, and P.F. Williams, *Digest of Tech. Papers, Eighth IEEE Int. Pulsed Power Conf.*, K. Prestwich and R. White eds., (IEEE, New York, 1991), pp. 1028-1031.
9. "Inhibition of Surface-Related Electrical Breakdown of Long p^+i-n^+ Silicon Structures," F.E. Peterkin, P.F. Williams, B.J. Hankla, L.L. Buresh, and S.A. Woodward, *Appl. Phys. Lett.* **62**, 2236-38 (1993).
10. "An Optical Technique for Measurement of Semiconductor Surface Electric Fields," H.P. Sardesai, W.C. Nunnally, and P.F. Williams, submitted to the Review of Scientific Instruments.
11. "Interferometric Determination of the Quadratic Electro-Optic Coefficient of Nitrobenzene," H.P. Sardesai, W.C. Nunnally, and P.F. Williams, submitted to Applied Optics/Optical Engineering.

5. PROFESSIONAL PERSONNEL

1. P.F. Williams, Ph.D., Lott Professor of Electrical Engineering, University of Nebraska-Lincoln
2. W.C. Nunnally, Ph.D., Associate Professor and Director of Applied Physical Electronics Research Center, University of Texas at Arlington.
3. James E. Thompson, Ph.D., Dean of Engineering, University of New Mexico, Albuquerque, NM
4. F.E. Peterkin, graduate research assistant (Ph.D.), University of Nebraska
5. W. Yi, graduate research assistant (Ph.D.), University of Nebraska
6. H.P. Sardesai, graduate research assistant (MS), University of Texas at Arlington
7. T. Vu, undergraduate research assistant, University of Texas at Arlington
8. B.J. Hankla, undergraduate research assistant, University of Nebraska
9. L.L. Buresh, undergraduate research assistant, University of Nebraska
10. S.A. Woodward, undergraduate research assistant, University of Nebraska
11. D.K. Scott, undergraduate research assistant, University of Nebraska
12. G.D. Cook, undergraduate research assistant, University of Nebraska
13. W.A. Machlab, undergraduate research assistant, University of Nebraska
14. D.G. Glenn, undergraduate research assistant, University of Nebraska

5.1 Advanced Degrees Awarded

1. Brian Lee Thomas was awarded the Ph.D. degree from the University of Texas at Arlington, December, 1989. The Thesis title was "Surface Flashover in Silicon Photoconductive Power Switches."
2. Harshad P. Sardesai was awarded the M.S. degree in Electrical Engineering by the University of Texas at Arlington, July, 1991. The thesis title is "Optical Measurements of Surface Electric Fields on Silicon Photoconductors."

6. INTERACTIONS

6.1 Meetings, Conferences, etc.

1. P.F. Williams gave a talk titled "A Mechanism for Surface Flashover of Semiconductors," at the Seventh Pulsed Power Conference, Monterey, CA, June 1989. W.C. Nunnally gave a talk titled "Recent Developments in the Investigation of Surface Flashover on Silicon Photoconductive Power Switches," at the Seventh Pulsed Power Conference, Monterey, CA, June 1989.
2. P.F. Williams gave a seminar titled "Physical Mechanisms of Surface Flashover on Silicon," to a group at N.S.W.C., Dahlgren, VA, on about July 31, 1990.
3. P.F. Williams gave a presentation titled "Physical Mechanisms of Surface Flashover on Silicon," at an SDIO review meeting held at Old Dominion University, Norfolk, VA, on about August 2, 1990. P.F. Williams gave a talk titled "Surface Flashover of Silicon at the S.P.I.E. OE/Boston '90 conference, held in Boston, MA on November 4, 1990.
4. W.C. Nunnally gave a talk titled "Surface Field Measurement of Photoconductive Power Switches using the Electro-optic Kerr Effect," at the S.P.I.E. OE/Boston '90 conference, held in Boston on November 4, 1990.
5. W.C. Nunnally gave a talk titled "Investigation of Surface Electric Fields Prior to Flashover on Silicon Switch," at the University of New Mexico, April 16, 1990.
6. W.C. Nunnally gave a talk titled "UT Arlington Photo-conductive Switching Research," at the Lawrence Livermore National Laboratory on May 31, 1990.
7. P.F. Williams gave a talk titled "Surface Flashover of Silicon" at the Eighth International Pulsed Power Conference, San Diego, CA June, 1991.
8. W.C. Nunnally gave a talk titled "Optical Measurements of Surface Fields on Silicon Photoconductive Power Switches," at the Eighth IEEE Pulsed Power Conference, June 17-19, 1991, San Diego, CA.
9. H.P. Sardesai gave a talk titled "Recent Developments in the Optical Measurements of Surface Electric Fields on Silicon Photoconductive Power Switches," at the S.P.I.E. International Symposium COET 91, held December 16-20, 1991, Bangalore, India.
10. P.F. Williams gave a talk titled "Surface Flashover of Silicon" at the Fourth SDIO/ONR Pulse Power Meeting held in Los Angeles, CA in June, 1991.
11. P.F. Williams gave a talk titled "Breakdown of High-Voltage Silicon Devices," at the Fifth SDIO/ONR Pulse Power Meeting held in Washington, DC in August 1992.